Original Article

Structural Health Monitoring

Structural Health Monitoring
1–27

DOI: 10.1177/1475921718760483
journals.sagepub.com/home/shm
SAGE

Real-time unified single- and multi-channel structural damage detection using recursive singular spectrum analysis

Basuraj Bhowmik[1], Manu Krishnan[2], Budhaditya Hazra[1] and Vikram Pakrashi[3]

Abstract

A novel baseline-free approach for continuous online damage detection of multidegree of freedom vibrating structures using recursive singular spectral analysis in conjunction with time-varying autoregressive modeling is proposed in this article. The acceleration data are used to obtain recursive proper orthogonal components online using rank-one perturbation method, followed by time-varying autoregressive modeling of the first transformed response, to detect the change in the dynamic behavior of the vibrating system from its original state to contiguous linear/nonlinear states indicating damage. Most work to date deal with algorithms that require windowing of the gathered data that render them ineffective for online implementation. Algorithms focused on mathematically consistent recursive techniques in a rigorous theoretical framework of structural damage detection are missing that motivates the development of the present framework. The response from a single channel is provided as input to the algorithm in real time. The recursive singular spectral analysis algorithm iterates the eigenvector and eigenvalue estimates for sample covariance matrices and new data point at each successive time instants. This eliminates the need for offline post processing and facilitates online damage detection especially when applied to streaming data without requiring any baseline data. Lower order time-varying autoregressive models are applied on the transformed responses to improve detectability. Numerical simulations performed on a five-degree of freedom nonlinear system and on a single degree of freedom system modeled using a Duffing oscillator under white noise excitation data, with different levels of nonlinearity simulating the damage scenarios, demonstrate the robustness of the proposed algorithm. The method further validated on results obtained from experiments performed on a cantilever beam subjected to earthquake excitation; a toy cart experiment model with springs attached to either side; demonstrate the efficacy of the proposed methodology as an appropriate candidate for real-time, reference-free structural health monitoring.

Keywords

Recursive singular spectral analysis, time-varying autoregressive modeling, damage-sensitive features, structural health monitoring, real-time damage detection

Introduction

Modern society is heavily dependent on structural and mechanical systems such as aircraft, bridges, power generation systems, buildings and defence systems. A significant portion of the aforementioned built infrastructure is distressed and in need of investment, while there is inadequate and limited resources to do so.[1] Operation, within and sometimes beyond the initially designed service life, requires assessment of the system in relation to performance metrices considering aging and degradation. This requirement leads to the need of

[1]Department of Civil Engineering, Indian Institute of Technology Guwahati, Guwahati, India
[2]Department of Aerospace and Ocean Engineering, Virginia Tech, Blacksburg, USA
[3]School of Mechanical & Materials Engineering, University College Dublin, Dublin, Ireland

Corresponding author:
Budhaditya Hazra, Department of Civil Engineering, Indian Institute of Technology Guwahati, Guwahati 781039, Assam, India.
Email: budhaditya.hazra@iitg.ernet.in

efficient damage detection techniques in order to detect and locate the damage, estimate the severity of the damage, and predict the useful remaining life of a structure. The term *structural health monitoring* (SHM) is related to the aforementioned objectives and often refers to the process of implementing damage detection strategies in structures involving the observation of a structure or mechanical system over time using periodically spaced response measurements, the extraction of damage-sensitive features (DSFs) from these measurements, and the statistical analysis of these features to determine the current state of system health.[2,3] Although damage detection strategies are well reported in the literature,[4–9] the evolution of real-time damage detection schemes capable of conducting baseline-free damage identification, in the backdrop of sparse and dense sensor economics, still remains a challenge. This is primarily due to the under-development of damage indicators capable of indicating damage instances and location of damage, simultaneously, in a single framework, and the complexities arising due to computational exhaustion that are memory and resource consuming. As the occurrence of damage can often be a real-time event,[4] changes in the DSFs can be efficiently evaluated recursively for continuously streaming data. This article addresses the key aspects of SHM that involves identifying the time of damage and detecting the precise location of damage in a structure in an online framework.

A majority of the damage detection schemes are offline in nature that analyze data in batches. Damage detection of structures in real time is a relatively new idea that requires significant development in the literature. Online damage detection entails identification of damage of a multi-degree-of-freedom (MDOF) vibrating system as the recorded vibration data streams in real time. Application of system identification–based SHM strategies utilizes advanced signal processing techniques[10] over vibration measurements gathered from a dense array of sensors[9] to monitor the condition of a structure. Numerous vibration-based damage detection methods have been developed in recent years which utilize changes in modal properties such as natural frequency,[5] damping,[5,11] and mode shapes[12] in order to detect damage resulting from various environmental conditions,[13] human-induced excitation or natural events[4,14] such as earthquake[15] and strong winds.[4,5] These damage detection techniques can be broadly classified as model-based methods which rely heavily on extensively calibrated finite element model (FEM) of a system,[16,17] thus rendering them computationally expensive. With increased computational cost,[16] modeling errors,[17,18] and choice of model parameters (such as model order, mass, stiffness, damping parameters),[18,19] the model-based methods are associated with disadvantages, which limit their applications for real-time damage detection. Contrary to these traditional approaches, response-based methods or the non-parametric methods[10,20–22] often overcome the aforementioned limitations by utilizing advanced signal processing techniques in conjunction with vibration measurements to monitor the condition of a structure.

The use of data-driven techniques developed in the field of classical time series analysis,[7] multivariate statistics,[23] and signal processing[15,21] ranging to diverse applicabilities like system identification, tool wear detection, and missing data recovery shows great potential in finding key patterns for appropriate prediction of such series.[24,25] Singular spectrum analysis (SSA),[24] a powerful technique developed in recent years, utilizes the key concept of separability for decomposition[24] and reconstruction of the time series[24,25] in two separate steps, without any statistical assumptions such as stationarity of the series and normality of the residuals. Due to the methodological stress on separability of one component of the series from another one, the assumption of stationarity is not required, making the algorithm amenable toward applicability for nonstationary time series as well. A useful tool in the predicting trends in time series, SSA can be used to address problems related to smoothing, extraction of seasonality components, optimal filtering, and analysis of seismic signals, using basis functions characterized by its data-adaptive nature. This makes the approach extended to the analysis of nonlinear aspects.[26] SSA decomposes a given time series into a set of additive time series and separates a multi-frequency signal into its simpler components. Using principal component analysis (PCA), the method projects an original time series onto a vector basis obtained from the series itself. In this process, the set of these series can be seen as a slowly varying trend representing the signal mean at each instant. As a result, the special features of the structure expressed by vibration signals in the signal and noise subspace can be extracted.[25]

The development of online damage detection techniques based on processing of response streaming in real time still remains a challenge. The main motivation behind the present work is to develop a *unified damage detection framework using single and multiple sensors* that can process data online and detect damage in a structure in real time. Applications involving aging and wearing out of components, processes dealing with seismic signals, are generally time-varying where the signals evolve in real time and the process becomes too complex to be analyzed via a simple offline method.[23,27] In practical SHM scenarios, data stream continuously in real time, which further necessitates that the algorithm should be amenable toward online implementation, independent of any baseline (reference) data. Traditional SSA requires a batch of data to elicit principal components (PCs) of the original time series, via

eigen decomposition of the covariance matrix that solely works offline. In this article, a baseline-free approach has been proposed which facilitates the monitoring of structural systems directly using acceleration data, based on recursive singular spectrum analysis (RSSA), as a tool for real-time processing of data. The proposed method uses first-order perturbation (FOP) approach for the Hankel covariance matrix estimate with every new sample obtained in real time. Whereas the traditional SSA approach processes chunks of data acquired in batch mode, RSSA provides online processing of data based on rank-one eigenvector updates in a recursive framework, as and when the data stream in real time.[8,28] Once the eigen space updates are obtained, an approximation of the original time series is carried out by reconstruction, where the framework then utilizes time-varying autoregressive (TVAR) modeling in conjunction with DSFs for identifying the instant of damage.[24]

Time series models work extremely well in capturing the key features of any data series, thus finding application in monitoring structural condition and detection of damage using time-varying coefficients, without resorting to spectral representation. Analysis of coefficients of autoregressive (AR) model,[2,7] autoregressive moving average (ARMA) model, and autoregressive moving average with exogenous input (ARMAX) model are some of the noteworthy aspects of traditional damage detection schemes extensively developed in the literature.[7,9] An inherent drawback of these methods is the fact that the methods are not receptive toward online implementation for a continuous real-time streaming of data. To tailor the basic AR modeling used in this article toward recursive implementation and to better capture the non-stationarity involved with the data due to the damage induced in the structure, the authors have resorted to TVAR modeling,[8] which is utilized to obtain the coefficients in real time to track the changes, indicative of an onset of damage. In the proposed method, TVAR modeling is applied on the reduced order responses obtained from the RSSA algorithm, rather than the raw vibration responses, which allows a relatively low order time series model to capture the dynamics of the structure in a recursive framework. The proposed framework, exclusive of baseline data, facilitates simultaneous spatio-temporal damage detection of a structure in real time, through the monitoring of the time-varying coefficients of the TVAR models.

The main contributions of this work are as follows: First, a novel framework has been provided using RSSA as a structural damage detection tool that works in real time as the data stream in. To the best knowledge of the authors, concepts utilizing RSSA in the purview of structural damage detection has so far not been explored. Additionally, since SSA is conceptually different from PCA due to the involvement of Hankel covariance matrices, recursive eigenvalue perturbation on Hankel covariance matrices is a significantly novel contribution and not a straightforward extension of FOP on covariance matrices as done in recursive principal component analysis (RPCA).[8,28] Second, damage can be inferred using TVAR model on the reduced order response obtained from RSSA algorithm in the order of about 15% for both global damage and local damage cases. This level of damage has not been reported in the literature so far. Third, simultaneous real-time spatial and temporal damage detection using a single framework is difficult. Finally, the authors have extended the utility of the proposed algorithm to assess damage detection using multi-channel singular spectrum analysis (MSSA) which is capable of identifying the dominant patterns in time as well as space. An extension of MSSA toward real-time damage detection, known as recursive multi-channel singular spectrum analysis (RMSSA), is a key entitlement of this article. The current work strives to unify real-time damage detection schemes through single sensor and multiple sensors in a single recursive framework. To the best of the knowledge of the authors, a comprehensive framework involving RSSA and RMSSA toward SHM has been barely reported in the literature so far.

The proposed method is applied for damage detection in a 5-DOF nonlinear base isolated system with the base modeled as a Bouc–Wen (B-W) model,[8,28] and a single-story system modeled with a Duffing oscillator at its base. These numerical results were complemented with experimental tests involving a toy cart setup modeled as a single-degree-of-freedom system (SDOF) attached to six springs, three on either side of the mass, excited using ground motion on an actuator table. The authors have also provided a separate experimental verification involving a cantilever beam model fixed to a base plate on a shake table and excited using ground motions of varying intensities to detect damage based on the nonlinearity provided by a rubber strip attached to the free end of the beam. Additionally, a section dedicated toward the applicability of the proposed method for real-time damage detection of large data sets is provided that deals with the combined earthquake and ambient vibration data obtained from the UCLA Factor Building.

Background

SSA is a non-parametric method that works well with arbitrary statistical processes and requires no prior assumptions about the stationarity, linearity, or normality of the data set. Somewhat similar to PCA-based

methods,[8,28] SSA projects the original time series into a smaller dimensional space which is composed of lagged signal components, while retaining most of the variance and the information associated with the particular data set.[24,29] The most prominent difference between the methods is that while in PCA, the singular value decomposition (SVD) is carried out predominantly on data gathered from a vibrating system; SSA utilizes the time history data obtained from each sensor and performs SVD on the Hankel matrix formed by the streaming data.[24] PCA re-expresses the original data into a transformed state of uncorrelated variables and estimates the covariance updates of the data set in growing windows or in batches that hinders its applicability toward online implementation. The superiority of SSA over the basic classical approaches is that the method decomposes a series into its component parts and reconstructs the series by leaving out the random (or noise) component behind. To tailor the traditional SSA method toward online implementation, an extension premised mainly on FOP techniques, known as RSSA, is proposed in this article that enables online spatio-temporal damage detection in a single framework.[30]

Basic SSA

The main objective of SSA is to decompose the original time series into a set of simpler components[24,25] from which three different characteristics can be extracted, namely *slowly varying trend, harmonic* (or *oscillatory*) component, and *noise*. According to Golyandina and Zhigljavsky,[25] trend components correspond to slow varying additive component of the series in which the oscillations are removed or smoothed. The harmonic series are periodic in nature which are either pure or amplitude modulated, while the noise component is any aperiodic series that does not affect the performance and/or functioning of the algorithm since it is removed during the reconstruction of the time series. The algorithm creates a Hankel matrix out of the time series itself by sliding a window that is shorter than the length of the time series. This process is known as *embedding*. The matrix is then decomposed into a number of elementary matrices of decreasing norm, through the process of *singular value decomposition* (SVD). *Grouping* is done by truncating the summation of the elementary matrices to yield an approximation of the original matrix, neglecting the irrelevant matrices which hardly contribute to the norm of the original matrix. This results in an approximated time series which is computed by taking the average of the diagonals, known as *reconstruction* or *diagonal averaging*. The above description is further explained through the following steps.[24,25]

Step 1: Embedding. Consider a real valued time series $Y_T = (y_1, ..., y_T)$[25] composed of vectors that indicate measurements from each sensor. Embedding converts the one-dimensional time series Y_T into a multi-dimensional series $(X_1, ..., X_K)$ with vectors, $X_i = (y_i, ..., y_{i+L-1})^T$, where L represents the window length and $K = T - L + 1$, where T corresponds to the number of sample points. The result of this step is the trajectory matrix $\mathbf{X} = [X_1, ..., X_K]$, the elements of which are given as

$$\mathbf{X} = \begin{pmatrix} y_1 & y_2 & y_3 & \cdots & y_K \\ y_2 & y_3 & y_4 & \cdots & y_{K+1} \\ y_3 & y_4 & y_5 & \cdots & y_{K+2} \\ \vdots & \vdots & \vdots & \ddots & \vdots \\ y_L & y_{L+1} & y_{L+2} & \cdots & y_T \end{pmatrix} \quad (1)$$

The result of this step is a Hankel matrix. At a snapshot of time, the number of rows of the matrix indicates the number of sensors corresponding to each DOF used for measuring the output vibration data, while the number of columns denotes the recorded data at each discretized sample point. The one time-dimensional time series is converted to a multi-dimensional series using a moving window of constant length. The choice of window parameters depends on the characteristics of data set.

Step 2: SVD on the Hankel matrix. The application of SVD on the Hankel matrix formed from the previous step has its roots in basic PCA. PCA is a linear orthogonal transformation that maps a set of physical variables to a new set of uncorrelated transformed variables, thereby resulting in reducing a complex data set to a lower dimension to reveal some hidden and simplified structures associated with the data set. PCA in the present context is carried out by performing an eigenvalue decomposition (EVD) on the Hankel covariance matrix, $\mathbf{C}_X = (1/N)\mathbf{X}\mathbf{X}^T$, where the superscript T indicates the transpose of the matrix. Let the EVD of the Hankel covariance matrix be written as $\mathbf{C}_X = \mathbf{U}\Upsilon\mathbf{U}^T$, where U represents the eigenvectors arranged row wise and Υ represents the diagonal matrix of eigenvalues in their descending order of significance.

Step 3: Eliciting PCs of the Hankel matrix. PCs are obtained by projecting the Hankel matrix onto the eigenvectors, thereby transforming the data set onto a new subspace. Let U_i represent the eigenvector corresponding to Υ_i eigenvalue. Selection of PCs is based on the relative

order of significance of eigenvalues. PC corresponding to a particular eigenvector is obtained as

$$\psi_i = (U_i^T)_{1\times L}(\mathbf{X})_{L\times K} \tag{2}$$

Once all the PCs are obtained, they can be arranged in a matrix of principal orthogonal components (POCs) as follows

$$\mathbf{\Psi} = [\psi_1, \psi_2, \ldots, \psi_L]^T \tag{3}$$

Step 4: Reconstruction of the Hankel matrix and the time series. The Hankel matrix may be expressed as the summation of d rank-one elementary matrices as $\mathbf{X} = \mathbf{R_1} + \mathbf{R_2} + \cdots + \mathbf{R_n}$, where n represents the number of non-zero eigenvalues in the Υ_i matrix. It should also be noted that the n elementary matrices are selected according to their relative order of significance as given by the decreasing order of their corresponding eigenvalues. The basic aim of this step is to reconstruct the Hankel matrix and thereby the original time series only using the PCs that explain maximum variance. This ensures elimination of noise and unwanted components from the time series, which further warrants the usage of a low model order in the succeeding steps. The elementary matrices are obtained by projecting the PCs back into the original eigen space as shown as follows

$$\begin{aligned} \mathbf{R}_i &= U_i \times \psi_i \\ \mathbf{X} &= \sum_{i=1}^{n} \mathbf{R}_i \end{aligned} \tag{4}$$

The Hankel matrix can now be reconstituted as per equation (4). The reconstituted trajectory matrix is an approximated version of the original matrix and the approximated time series is recovered by taking the average of the diagonals. Let x_{ij} be the elements of the Hankel matrix, where i denotes the row number and j denotes the column number. Considering $L^* = min(L, K)$, $K^* = max(L, K)$, and $T = L + K - 1$, it could be assumed that $x_{ij}^* = x_{ij}$ if $L < K$ and $x_{ij}^* = x_{ji}$, otherwise. The individual elements of the time series X_k are obtained using the following equations[24,25]

$$x_k = \begin{cases} \frac{1}{k+1}\sum_{m=1}^{k+1} x^*_{m,k-m+2} & for\ 0 \leqslant k < L^* - 1 \\ \frac{1}{L^*}\sum_{m=1}^{L^*} x^*_{m,k-m+2} & for\ L^* - 1 \leqslant k < K^* \\ \frac{1}{T-k}\sum_{m=k-K^*+2}^{T-K^*+1} x^*_{m,k-m+2} & for\ K^* \leqslant k \leqslant T \end{cases} \tag{5}$$

From the formulations involved, it is clear that the regular SSA requires a batch of data. These data provide a covariance matrix via the trajectory matrix of the signal in an offline framework. By the subsequent application of SVD on the covariance matrix, the PCs of the time series are elicited. This part requires exhaustive matrix operations and makes the SSA unsuitable for online applications.

Recursive singular spectrum analysis (RSSA)

The main disadvantage of traditional SSA is that it analyzes data in batches, offline. Recent research in signal processing and information technology has identified SSA as an efficient damage detection tool,[30] leading to the development of SSA-based structural damage detection algorithms.[31,32] The major challenge toward tailoring SSA toward an online implementation is to perform the EVD of the Hankel covariance matrix at each time instant, which can be time-consuming, thereby impeding its practical applicability toward real-time damage detection. This can be alleviated through the use of FOP approach,[28,33] which provides recursive updates of eigen subspace from the previous eigen space of the data at a particular time instant.

For structural systems dealing with data evolving from zero-mean processes, the recursive estimation of the Hankel covariance matrix ($\mathbf{C}_k$) at any instant k can be structured in terms of the current sample vector (X_k) and the previous covariance estimates ($\mathbf{C}_{k-1}$) as follows

$$\mathbf{C}_k = \frac{k-1}{k}\mathbf{C}_{k-1} + \frac{1}{k}X_k X_k^T \tag{6}$$

However, for nonstationary data sets, the recursive mean at each instant of time needs to be accounted for in the estimation of the covariance matrix. The recursive mean at kth instant, μ_k, depends on the mean at the previous instant through the relation: $\mu_k = (k-1/k)\mu_{k-1} + (1/k)X_k$. The covariance estimate for cases involving mean shift can be expressed as $\tilde{\mathbf{C}}_k = (k-1/k)\mathbf{C}_{k-1} + (1/k)[X_k - \mu_k][X_k - \mu_k]^T$. In SHM problems, the dynamics of the system evolve predominantly from zero-mean processes. Damage detection formulations premised on recursive correction updates of the covariance matrix generally assume to ignore the local non-zero means at each time instant. Case studies from previously published works[8,28] as well as the current work reveal that the aforesaid assumption does not hinder the practical applicability of the online damage detection algorithms. The incorporation of $\tilde{C}$ in the formulation of the covariance estimate is therefore inconsequential. Henceforth, for the remainder of the draft, $\tilde{C}$ has been dropped for subsequent formulation and analysis. However, a simple case study involving mean shift for covariance estimate is provided in the later stages of the draft (section "Temporal damage detection results"), which shows that the incorporation of mean shift does not alter the results significantly. A

comprehensive extension of the proposed algorithm involving mean shifts will be taken up as a future work backed with extensive numerical verifications and proper experimental setups.

The current L dimensional sample vector ($X_k = [x_{k-L+1}, x_{k-L+2}, x_{k-L+3}, \ldots, x_k]^T$) comprises L lagged elements of the one-dimensional time series, L being the initial signal length. The objective of preselecting a desired initial signal length is to preserve the components with most of the damage information (by selecting components with higher singular values to retain the trend and oscillatory parts) and to eliminate the components of less significance such as noise. The covariance estimate at kth instant can be written in terms of eigenvalue and eigenvector matrix at a particular time instant as $\mathbf{C}_k = \mathbf{U}_k \Upsilon_k \mathbf{U}_k{}^T$ with $\varpi_k = \mathbf{U}_{k-1}^T \mathbf{X}_k$, as the projection of the sample vector into the previous eigen subspace. Substituting these expressions in equation (6), the following equation is obtained

$$\begin{aligned}\mathbf{U}_k(k\Upsilon_k)\mathbf{U}_k^T &= (k-1)\mathbf{U}_{k-1}\Upsilon_{k-1}\mathbf{U}_{k-1}^T + \varpi_k\varpi_k^T\mathbf{U}_{k-1}\mathbf{U}_{k-1}^T \\ &= \mathbf{U}_{k-1}\{(k-1)\Upsilon_{k-1} + \varpi_k\varpi_k^T\}\mathbf{U}_{k-1}^T\end{aligned} \tag{7}$$

In the above expression, with a finitely large sample size (k) and low damping estimates,[28] the term $((k-1)\Upsilon_{k-1} + \varpi_k\varpi_k^T)$ generally shows a diagonally dominant behavior. The diagonal dominant structure of this term ensures the application of Gershgorin's theorem,[34] rendering in the application of FOP approach admissible to obtain the eigenvalues and eigenvectors. Interested readers could refer Krishnan et al.[28] and Li et al.[33] for details. The application of Gershgorin's theorem ensures the EVD of the term to be of the form $\mathrm{P}_k\mathbf{\Gamma}_k\mathrm{P}_k^T$, where $\mathbf{P}$ is orthonormal and $\mathbf{\Gamma}$ is diagonal. Substituting the EVD in place of $((k-1)\Upsilon_{k-1} + \varpi_k\varpi_k^T)$ in equation (7), a new formulation is obtained as follows

$$\mathbf{U}_k(k\Upsilon_k)\mathbf{U}_k^T = (\mathbf{U}_{k-1}\mathrm{P}_\mathbf{k})\mathbf{\Gamma}_k(\mathrm{P}_\mathbf{k}^\mathbf{T}\mathbf{U}_{k-1}^T) \tag{8}$$

From equation (8), recursive updates of the eigen subspace are obtained as a function of the previous eigen space as

$$\begin{aligned}\mathbf{U}_\mathbf{k} &= \mathbf{U}_{k-1}\mathrm{P}_\mathbf{k} \\ \Upsilon_k &= \frac{\mathbf{\Gamma}_k}{k}\end{aligned} \tag{9}$$

Equation (9) provides an iterative relation between eigen spaces at consecutive time instants. On using FOP approach, the recursive eigenvectors obtained at each time instants are not ordered in the same sequence as the previous time instant, thus presenting the problem of permutation ambiguity. This can be resolved by arranging the obtained eigenvectors according to the decreasing order of the corresponding eigenvalues in $\mathbf{\Gamma}_k$. For the working of RSSA algorithm, this is one of the key steps as eigenvalues of the covariance Hankel matrix need to be ordered before proceeding with the evaluation of PCs and reconstruction of Hankel matrix using them. The contribution factor for a particular ith eigenvector U_i is given by $\beta_i^2 / \sum_{i=1}^n \beta_i^2$, where β_i^2 is the eigenvalue corresponding to U_i. After obtaining the eigen space updates at a particular time instant from the previous eigen space and current sample vector, PC values of the time series at a particular time series can be extracted as follows

$$\psi_i(k) = (U_i^T(k))_{1\times L}(\mathbf{X}_k)_{L\times 1} \tag{10}$$

Using the above equation, the i^{th} PC value at particular time instant is obtained. Depending upon the relative contribution of the eigenvectors, the number of PCs required for reconstruction can be automated. For the present work, at any instant k, the PCs of eigenvectors that explain more than 90% of the system's variance is used for reconstruction. In the reconstruction step, the ith PCs are projected back into its original subspace to obtain last column of the corresponding elementary matrix

$$\mathbf{R}_i(k) = (U_i(k))_{L\times 1} \times (\psi_i(k))_{1\times 1} \tag{11}$$

It is to be noted here that the last entry of the $\mathbf{R}_i(k)$ vector, denoted here as $r_i(k)$, is used to obtain the value of the reconstructed time series entry at the kth instant of time as shown as follows

$$x(k) = \frac{1}{n}\sum_{i=1}^{n} r_i(k) \tag{12}$$

where n denotes the number of eigenvalues explaining more than 90% of the variance. The reconstructed signal values as per equation (12) is recursively obtained at each instant of time as and when the vibration data stream in. The importance of this reconstructed signal is that it has simpler components, making it amenable toward a lower AR order model, deemed sufficient[7,8] to capture the dynamics of the structure, and more sensitive toward singular events like damage. TVAR modeling is subsequently performed on this reconstituted signal.

Recursive damage indices

In the present framework, RSSA facilitates online processing of data producing recursive updates of eigenvectors and eigenvalues, referred to as eigen subspace. The eigen subspace by themselves cannot detect the change in system properties inflicted due to damage, if not processed by a set of damage markers commonly referred to as DSFs.[15] The primary requirements of

good DSFs are their ability to detect the presence of damage, effectively distinguish between the damaged and undamaged states of the structure, followed by their capacity to possibly locate and quantify the extent of damage. Additionally, to detect damages in real time, the proposed DSFs should be amenable toward online implementation and should accurately identify the presence of damage as and when the response data stream in continuously. Several damage detection and SHM techniques have been proposed in the literature[2] that involve use of specific DSFs whose changes signify damage to the system. The disadvantages associated with traditional DSFs include requirement of (1) baseline or reference data from a healthy structure, (2) windowing of response data, and so on, which impedes their application in an online framework. In this section, a brief background on the formulation of *online DSFs* is proposed utilizing the concepts of TVAR coefficients and recursive signal statistics. These features are based on the reorientation of eigen space due to damage manifested in the form of change in the pattern of TVAR modeling before and after damage. In the following sections, TVAR coefficients (a_i), and eigen ratio difference (ERD) for damage detection, are presented.

TVAR coefficients

The key DSFs utilized in the paper are the TVAR coefficients. The motivation for this DSF is derived from the use of AR coefficients as a criterion for novelty evaluation,[35] which presents the use of a statistical parameter known as Mahalanobis distance applied on AR coefficients to distinguish between a damaged state and an undamaged state. In order to characterize the behavior of the POC updates (which can be approximated to normal coordinates), TVAR modeling is adopted here.[8] The use of TVAR modeling for detecting structural damages has been attempted in the recent times with a fair amount of success.[36] TVAR coefficients of the modeled transformed response are tracked in real time in order to identify the damage instant. However, estimation of these coefficients frequently requires the use of windowing and baseline data to detect damage, making online implementation difficult. These drawbacks motivate the need of using a TVAR modeling–based framework,[36] which does not involve any baseline to detect damage in real time, enabling it to capture the nonstationary nature associated the data due to damage. The proposed method tracks the TVAR coefficients in real time, which are used to ascertain damage induced in the structure by a change in the mean level of the plot, at the exact instant of damage. The sudden changes in TVAR coefficients indicate the alterations in the dynamical properties of the system, such as shifts in natural frequencies, changes in the mode shapes of the system, induced due to damage in the system. In the proposed work, the transformed response (i.e. the first POC) extracted from the RSSA algorithm is modeled using a TVAR model. However, the main drawback associated with using TVAR models is the selection of model order apriori such that the resulting TVAR model correctly characterizes the data during the times of interest. The use of POCs instead of the raw vibration data, whose near resemblance to normal coordinates enables the use of a low model order, resolves the issue of model order selection. As the transformed response consists of a simpler components, it ensures that low model order is sufficient to capture its dynamics; therefore, in the proposed framework, a model order of 2 (two) is pre-selected for all cases.

Let $X(k)$ represent the reconstructed signal at any instant which captures the maximum kinetic energy of the system and let $V(k)$ denote a zero-mean Gaussian white noise with variance σ_v^2. Then the AR model of order p can be represented as

$$X(k) = \sum_{i=1}^{p} a_i X(k-i) + V(k) \tag{13}$$

For real-time implementation of AR model and also to make it robust against nonstationarities that might be encountered in real-life data (e.g. earthquake excitation, real-time occurrence of damage), the POCs are modeled using TVAR modeling in which a_i's is a function of time. For this purpose, the Kalman filter is utilized to estimate these time-varying coefficients.[36] The following equation is the discrete representation of the $a_i(t)$ coefficients and $W(k)$ is the process noise with variance σ_w^2 and covariance, $\mathbf{P_w} = \mathbf{I_{p\times p}}\sigma_w^2$. Both noise measurements $V(k)$ and $W(k)$ are mutually independent and uncorrelated. Consider the following set of equations, where the unknown state vector $B(k)$ is expressed as shown

$$\begin{aligned} B(k) &= \mathbf{\Gamma}(k-1)B(k-1) + W(k) \\ X(k) &= \mathbf{C(k)}B(k) + V(k) \end{aligned} \tag{14}$$

The state vector $B(k)$ is given by $B(k) = [a_1(k), a_2(k), \ldots, a_p(k)]^T$. The matrix $\Gamma(k-1)$ is an identity matrix ($\mathbf{I}_{p\times p}$). The matrix C_k is the observation data with discrete k steps given as: $\mathbf{C}(k) = [X(k-1), X(k-2), \ldots, X(k-p)]$. The Kalman filter has mainly two processes: one is the stepwise time update (prediction) and the other one is measurement update (correction) of the predicted data. At each step, the set of the Kalman filter equations can be written as Hazra et al.[36]

$$\begin{aligned} B(k|k-1) &= B(k-1|k-1) \\ \mathbf{P}_b(k|k-1) &= \mathbf{P}_b(k-1|k-1) + \mathbf{I}\sigma_w^2 \\ \psi^1(k|k-1) &= \mathbf{C}(k)B(k|k-1) \\ \sigma_x^2(k|k-1) &= \mathbf{C}(k)\mathbf{P}_b(k|k-1)\mathbf{C}(k)^T + \sigma_v^2 \end{aligned} \tag{15}$$

And

$$\begin{aligned} \mathbf{KG}(k) &= \mathbf{P}_b(k|k-1)\mathbf{C}(k)^T\sigma_x^2(k|k-1)^{-1} \\ B(k|k) &= B(k|k-1) - \mathbf{KG}(k)[X(k) - X(k|k-1)] \\ \mathbf{P}_b(k|k) &= [\mathbf{I} - \mathbf{KG}(k)\mathbf{C}(k)]\mathbf{P}_b(k|k-1)] \end{aligned} \tag{16}$$

where $B(k|k-1)$ represents apriori estimate and its linear combination would result in $B(k|k)$, which is aposteriori. The Kalman gain $\mathbf{KG}(k)$ gives a weightage to the prediction error $X(k) - X(k|k-1)$, to minimize the state estimation error $B(k|k)$. The apriori and the posteriori covariance estimates are given by $\mathbf{P}_b(k|k-1)$ and $\mathbf{P}_b(k|k-1)$, respectively. Although the TVAR model facilitates adequate representation of the nonstationary transformed response, however, in order to use it for damage detection, the TVAR model alone is not enough. Consequently, DSFs are applied on the TVAR coefficients to detect damage which run in real time. The basic equation (13) therefore becomes

$$X(k) = a_1(k)X(k-1) + a_2(k)X(k-2) + V(k) \tag{17}$$

where $X(k)$ represents the POC at any instant that captures the maximum variance of the system. Although a_1 and a_2 are expected to alter mildly at each time instants due to a drift in the post damage values from the predamage values, the damage instant is characterized by sudden changes in the overall behavior of TVAR coefficients. The change in a_1 and a_2, tracked recursively, serves as an indicator of damage.

Damage detection using recursive eigen ratio difference

In the present work, the ratio of two singular values, quantifying the coupling level between two singular values in RSSA, is utilized as a secondary DSF. The use of this quantity as a possible indicator of instability was first adopted for monitoring volcanic activity.[37] The principle behind the use of this marker is that structural damage or instability induces a low frequency component in the signal, creating a decoupling between the two most significant PCs. This decoupling can intuitively be represented in the form of ratio between their corresponding singular values and eigenvalues. This concept of decoupling has been utilized in the present work to formulate an online damage index known as recursive eigen ratio difference to accurately identify the instant of damage, which is given as follows

$$\delta(k) = \left[\frac{(\lambda_1(k) - \lambda_2(k))}{\sum_{i=1}^{L} \lambda_i} \right] \tag{18}$$

At the instant of damage, recursive ERD shows an alteration in its mean level to indicate the decoupling between the two most significant singular values. The potential of ERD to be implemented online toward damage detection demonstrates its capability to detect damage even for cases of a nonstationary nature of input data. ERD when examined in a recursive framework supplements the use of AR coefficients as an effective damage detection tool for the proposed framework. This is shown at a later stage of the manuscript.

Multichannel singular spectrum analysis (MSSA)

This section describes the basic MSSA and its recursive implementation, suitable for online implementation. MSSA is a data-driven technique arising from research on alternative tools for the analysis of multi-channel time series and can be considered as a natural extension of the basic SSA algorithm.[38] SSA, albeit being an efficient algorithm for extracting the principal patterns in time, becomes computationally demanding for structures with significantly large number of DOF (e.g. UCLA Factor Building (UCLAFB)).[28] MSSA uses a multivariate time series with all state variables of the coupled systems in the construction of the augmented trajectory matrix. The literature in MSSA[38,39] shows that the variable chosen to analyze the system will have significant impact on the robustness of the algorithm to capture the dynamics of the system under study. The conventional eigenvector or PCA is a special case of the MSSA when no time lags are introduced. According to Richman,[40] the eigenvectors show distortions that contribute to inaccurate representation of the physical relationships in the data. In the presence of data gaps in the data series, the resulting modes of the decomposition of the data are not strictly orthogonal.[41]

Consider the multivariate time series of length N and D channels, $\mathbf{x} = \{\mathbf{x}_n^d : d = 1, ..., D; n = 1, ..., N\}$. Similar to SSA, the first step of MSSA algorithm is to create an augmented trajectory matrix with data from the concerned channels. Each channel d is embedded into an L dimensional phase space using lagged replicates $X_1^i, X_2^i, ..., X_k^i$, where i ranges from 1 to D, D being the number of channels considered for MSSA. Hence if there are D channels, each embedded into an L dimensional phase space system, the number of rows of the augmented matrix will be $L \times D$ and number of columns will be $K = N - L + 1$. The structure of the trajectory matrix is shown as follows

$$\mathbf{X}_D = \begin{bmatrix} \underbrace{\begin{matrix} x_1^1 & x_2^1 & x_3^1 & . & x_L^1 \\ x_2^1 & x_3^1 & x_4^1 & . & x_{L+1}^1 \\ . & . & . & . & . \\ . & . & . & . & . \\ x_K^1 & x_{K+1}^1 & x_{K+2}^1 & . & x_N^1 \end{matrix}}_{Channel-1} & \underbrace{\begin{matrix} x_1^2 & x_2^2 & x_3^2 & . & x_L^2 \\ x_2^2 & x_3^2 & x_4^2 & . & x_{L+1}^2 \\ . & . & . & . & . \\ . & . & . & . & . \\ x_K^2 & x_{K+1}^2 & x_{K+2}^2 & . & x_N^2 \end{matrix}}_{Channel-2} & \cdots & \underbrace{\begin{matrix} x_1^D & x_2^D & x_3^D & . & x_L^D \\ x_2^D & x_3^D & x_4^D & . & x_{L+1}^D \\ . & . & . & . & . \\ . & . & . & . & . \\ x_K^D & x_{K+1}^D & x_{K+2}^D & . & x_N^D \end{matrix}}_{Channel-D} \end{bmatrix}^{\mathbf{T}} \tag{19}$$

The formulation for MSSA is similar to the steps provided in section "Basic SSA," for a basic SSA algorithm. Applying SVD on the augmented trajectory covariance matrix yields $L \times D$ eigenvalues and eigenvectors. As the number of channels increases, MSSA becomes computationally expensive. However, MSSA shows good results in interpreting damage events, which is illustrated in the later parts of the study. Hence, projecting the data set onto the eigenvectors simplifies the picture of a possibly high dimensional complex system by viewing it in an optimal subspace.[42] It is well understood that there will be D sets of $L \times L$ eigenvalue matrix and eigenvector matrix. Consequently, there will be D sets of L PCs, each accounting for correlation between different data sets taken as input to the algorithm. For TVAR modeling, only one signal is required, but MSSA algorithm gives D reconstructed signals as output. Hence, to tailor the basic MSSA algorithm toward damage detection using TVAR modeling, the authors suggest utilizing the first two PCs of every D channels, toward building a composite signal that accounts for all the D input channels. The composite signal contains the maximum information to aid toward the detection problems, obtained using the most significant PCs. Let $\mathbf{\Psi}_D = [\psi_1^1, \psi_2^1, \ldots, \psi_L^1, \ldots, \psi_1^D, \psi_2^D, \ldots, \psi_L^D]^{\mathbf{T}}$ represent the PCs obtained from Step 3 as mentioned in section "Basic SSA." Using only the first two PCs of each channel, the trajectory matrix is reconstructed as follows

$$\mathbf{R}_i = \frac{\left\{ \sum_{j=1}^{D} \sum_{i=1}^{2} U_i^j \times \psi_i^j \right\}}{D} \tag{20}$$

The composite signal from the trajectory matrix is obtained using the same diagonal averaging as explained in equation (5). The reconstructed composite signal has the maximum information contained toward TVAR modeling and subsequent damage detection. The signal is generated based on the PCs containing the maximum variance, in each channel.

RMSSA

The main disadvantage of MSSA algorithm is that when the number of channels increases, it becomes computationally more involved. This becomes an impeding factor even for developing a recursive version of basic MSSA algorithm toward processing real-time MDOF data. The authors have made an attempt to develop a recursive version of MSSA algorithm in this article by modifying the basic RSSA algorithm to account for multiple input channels, which is a key entitlement of the paper. Following the similar lines of development, as in equation (6), the RMSSA algorithm can be proposed as follows

$$\mathbf{C_k} = \frac{k-1}{k}\mathbf{C_{k-1}} + \frac{1}{k}\widetilde{X}_{k_D}\widetilde{X}_{k_D} \tag{21}$$

where $\widetilde{X}_{k_D} = [x_{k-L+1}^1, x_{x-L+2}^1, x_{x-L+3}^1, \ldots, x_k^1, \; x_{k-L+1}^2, x_{x-L+2}^2, x_{x-L+3}^2, \ldots, x_k^2, \ldots, x_{k-L+1}^D, x_{x-L+2}^D, \; x_{x-L+3}^D, \ldots, \; x_k^D]^T$. Once the recursive equation is ready, all the other steps from equation (7) to equation (12) follow. The key steps of the formulation include the updating of the covariance matrix formed at each time stamp and providing eigen decomposition so as to tailor the basic MSSA algorithm toward its recursive version. As discussed in the preceding sections, the proposed algorithm could be applied for nonstationary cases involving mean shift as well. The recursive update of the covariance matrix could be expressed as $\tilde{\mathbf{C}}_k = (k-1/k)\mathbf{C}_{k-1} + (1/k) \; [\tilde{X}_{k_D} - \mu_k] \; [\tilde{X}_{k_D} - \mu_k]^T$, where the recursive mean at each instant of time, $\mu_k = (k-1/k)\mu_{k-1} + (1/k)\tilde{X}_{k_D}$. As the data evolve from zero-mean process, following similar lines of development, the eigen decomposition of the covariance matrix at the kth time instant could be written as $\mathbf{C}_k = \mathbf{W}_k \mathbf{\Omega}_k \mathbf{W}_k^T$. On substituting to the covariance update equation (21), with $\beta_k = \mathbf{W}_{k-1}\tilde{X}_{k_D}$, and performing simple algebraic calculations, the following equation is obtained

$$\mathbf{W}_k \Omega_k \mathbf{W}_k^T = \mathbf{W}_{k-1}\left[(k-1)\Omega_{k-1} + \beta_k \beta_k^T\right]\mathbf{W}_{k-1}^T \tag{22}$$

For finitely large sample size k and low damping estimates,[28] the term $((k-1)\Omega_{k-1} + \beta_k \beta_k^T)$ generally shows a diagonally dominant behavior. The diagonal dominant structure of this term ensures the application of Gershgorin's theorem, rendering in the application of FOP approach admissible to obtain the eigenvalues and eigenvectors.[28,33] The application of Gershgorin's theorem ensures the EVD of the term to be of the form

$T_k \Lambda_k T_k^T$, where $\mathbf{T}$ is orthonormal and Λ is diagonal, similar to the previous approach. Substituting the EVD in equation (22), the covariance matrix update could be simplified as follows

$$\mathbf{W}_k k \Omega_k \mathbf{W}_k^T = (\mathbf{W}_{k-1}\mathbf{T}_k)(\Lambda_k)(\mathbf{W}_{k-1}\mathbf{T}_k)^T \tag{23}$$

which yields the following iterative update equations

$$\left.\begin{array}{l} \mathbf{W}_k = \mathbf{W}_{k-1}\mathbf{T}_k \\ \Omega_k = \frac{\Lambda_k}{k} \end{array}\right\} \tag{24}$$

Equation (24) provides an iterative relation between eigen spaces at consecutive time instants. Following a similar approach as discussed in section "RSSA," the PC values of the time series at a particular time series can be extracted as follows

$$\psi_i(k) = (W_i^T(k))(\mathbf{X}_{k_D}) \tag{25}$$

The recursively updated trajectory matrix is reconstructed by utilizing the first two signal PCs of all the D input channels as shown as follows

$$\mathbf{R}_i(k) = \frac{\left\{\sum_{j=1}^{D}\sum_{i=1}^{2} W_i^j(k) \times \psi_i^j(k)\right\}}{D} \tag{26}$$

The composite signal value at kth instant of time is obtained as explained in equation (12). This is subsequently utilized for TVAR modeling to track DSFs in real time.

Proposed RSSA-based framework

The overall methodology followed in the paper entails a fine blend of separate modules that detect two key ingredients: *temporal* and *spatial* damage detection, simultaneously, in a single framework. The first module deals with the temporal damage detection, where the raw acceleration data are processed by the RSSA algorithm as the data stream in real time. This accounts for an online global damage detection framework as the data are not gathered in batches to form a baseline. TVAR modeling is carried out on the updated first PC, yielding TVAR coefficients at each instant of time. As previously explained, these TVAR coefficients are tracked online for any major and minor changes. DSF such as recursive ERD is utilized to further validate the instant of damage, obtained from the AR coefficients. Once the damage instant is detected, the spatial damage detection module further resolves the location of damage. The basic steps of the algorithm are enumerated as follows:

1. First, traditional SSA is employed on some initial data points (around 100 in number) in order to estimate the initial eigenvector and eigenvalue matrices. The number of data points chosen here is arbitrary and considered only to stabilize the algorithm for subsequent real-time damage detection.
2. The RSSA algorithm then operates online on the real-time input of the streaming data. This generates a Hankel matrix out of the set of physical responses.
3. Using the recursive gain depth parameter, the covariance estimate of the Hankel matrix at the present time instant is derived using the covariance estimate at preceding time instant. From the recursive updates, the eigenvector and eigenvalue matrices are updated using FOP approach and the transformed responses (PCs) are obtained using the RSSA algorithm.
4. During the reconstruction phase, an approximate time series is obtained according to the relative order of significance as given by the decreasing order of the corresponding eigenvalues.
5. The proposed time series models are generated based on the approximated time series and a TVAR model is fit. The DSFs are tracked real time in order to extract the changes in the model coefficients, thereby revealing the faults in the system.
6. Once the instant of damage is determined, the algorithm shifts on to the next module where the spatial detection of damage takes place. DSFs are tracked online, recursively, to capture the spatial effect of the damage. To further validate the instant of damage obtain from the AR plots, recursive ERD is utilized to show changes in the mean level at the instant of damage.

The flowchart shown in Figure 1 outlines the proposed damage detection scheme. Vibration responses are processed by the RSSA algorithm to obtain the transformed responses and TVAR modeling is utilized to extract time-varying coefficients through which damage instant is detected. It should be noted that the aforementioned proposed algorithm has the following characteristics: (1) the data are processed at each time instant, as and when it becomes available, that is, the algorithm works online; (2) to locate the instant of damage, a reference value (baseline) is not required, that is, it is baseline free; (3) there are no parameters controlling the working of the algorithm, hence its parameter free. These characteristics make it an appropriate choice for a real-time damage detection framework.

Numerical example

The applicability of the proposed method toward simulated models clearly exhibits the potential of the algorithm toward real-time damage detection. Numerical simulations are carried out on a four-story structure modeled with a B-W oscillator at its base and a single-story model with a Duffing oscillator. The global damage in the models is introduced through a change in the nonlinear force term governing the equation of motion. This is verified in the study through the use of a damage index (DI)[8,28] and validated through hysteresis plots, described in the following sections. The variations in the hysteresis plots closely resemble to the real-life occurrence of earthquakes, where the force–displacement graphs deviate due to the presence of damage. A stationary zero-mean Gaussian white noise sampled at 50 Hz for a duration of 50 s is used. Toward this, the models are described in detail followed by the detailed analysis of the results.

Description of the five-story structure with B-W isolator at its base

The five storied structure is modeled with four floors having linear stiffness and a nonlinear B-W isolator lumped at the base. The model under study is adapted from Krishnan et al.[28] A lead rubber bearing (LRB) isolator separates the base from the surrounding ground. The equation of motion for the system can be summarized as

$$\mathbf{M}\ddot{X} + \mathbf{C}\dot{X} + \mathbf{K}X = F - \mathbf{MI}\ddot{\mathbf{X}}_g \tag{27}$$

M, **C**, and **K** are the assembled mass, damping, and stiffness matrices, respectively. A simple shear building representation is assumed to arrive at the expressions for **M**, **C**, and **K** as per Krishnan et al.,[28] which can be referred for detail. The state equations for this system subjected to an external excitation vector W can be written as

$$\begin{aligned} \dot{X} &= \mathbf{A}X + \mathbf{E}W \\ Y &= \mathbf{B}X \end{aligned} \tag{28}$$

Here, the vector X is the vector of states, defined as the smallest possible subset of system variables that can represent the entire state of the system at any given time. The vector Y represents the output vector, which is governed by the **B** matrix. The system matrix, **A**, the excitation matrix **E**, and the observation matrix **B** are given by

$$\begin{aligned} \mathbf{A} &= \begin{bmatrix} [\mathbf{0}]_{5\times5} & [\mathbf{I}]_{5\times5} \\ -\mathbf{M}^{-\mathbf{I}}\mathbf{K} & -\mathbf{M}^{-\mathbf{I}}\mathbf{C} \end{bmatrix} \\ \mathbf{E} &= \begin{bmatrix} 0 & 0 & 0 & 0 & 0 & -\frac{1}{m} & -\frac{1}{m} & -\frac{1}{m} & -\frac{1}{m} & -\frac{1}{m} \end{bmatrix}^T \\ \mathbf{B} &= \begin{bmatrix} [\mathbf{I}]_{5\times5} & [\mathbf{0}]_{5\times5} \\ -\mathbf{M}^{-\mathbf{I}}\mathbf{K} & -\mathbf{M}^{-\mathbf{I}}\mathbf{C} \end{bmatrix} \end{aligned} \tag{29}$$

Numerical simulations are carried out on a simple 5-DOF mass, spring, and dashpot system. The mass at each of the four floor levels from the top is 7461 kg and at the base is 6800 kg. The damping coefficients for each floor level above the base are 23.71 and 3.74 kNs/m for the base. The stiffness coefficients for each of the floors above the base are 11,912 kN/m and that for the base is 232 kN/m.[28]

In equation (27), I is a vector with all elements unity and $\ddot{\mathbf{X}}_\mathbf{g}$ represents the ground acceleration. The vector X represents the displacement of each floor and the base, with X_4 being the displacement of the top floor. It should be noted that the forces due to base damping and stiffness terms (k_b and c_b) have been included in the nonlinear force (F) due to the LRB base isolator, which can be expressed as

$$F = \kappa z Q_{pb} + k_b X_b + c_b \dot{X}_b \tag{30}$$

where $Q_{pb} = (1 - k_{yield}/k_{initial})Q_y$ and k_b and c_b are the stiffness and the viscous damping, respectively, in the horizontal direction. The term $k_{initial}$ is the initial shear stiffness and k_{yield} is the post-yield shear stiffness of the LRB. The evolutionary variable z is used to provide the hysteretic component of the horizontal force, $Q_{hyst} = zQ_{pb}$. The variable z can be obtained by solving the following nonlinear differential equation

$$z = -\gamma z\left|\dot{X}_b\right|\left|z^{n-1}\right| - \beta\dot{X}_b|z^n| + A\dot{X}_b \tag{31}$$

where γ, β, A, and n are the shape parameters of the hysteresis loop.[28] For the current model, $A = \left(k_{yield}/k_{initial}\right)$, $\gamma = \beta$, and $n = 1$. The yield force Q_y is selected as 5% of the total weight of the building which gives $Q_y = 17,800$ kg and pre-yield to post-yield stiffness ratio $(k_{yield}/k_{initial}) = 1/6$. For the present study of the model, $\gamma = \beta = 39.1$. The constant κ controls the nonlinearity introduced into the equation of motion of the system (through the nonlinear force term). For instance, a change in κ from 1 to 0.4 is conveniently assumed as a 60% change in nonlinear characteristics of the system. The variations in the force–displacement characteristics replicate to instances of real-life occurrence of earthquakes where the hysteresis plots deviate due to the presence of damage, thus verifying the fact that the change in the nonlinear force term induces a

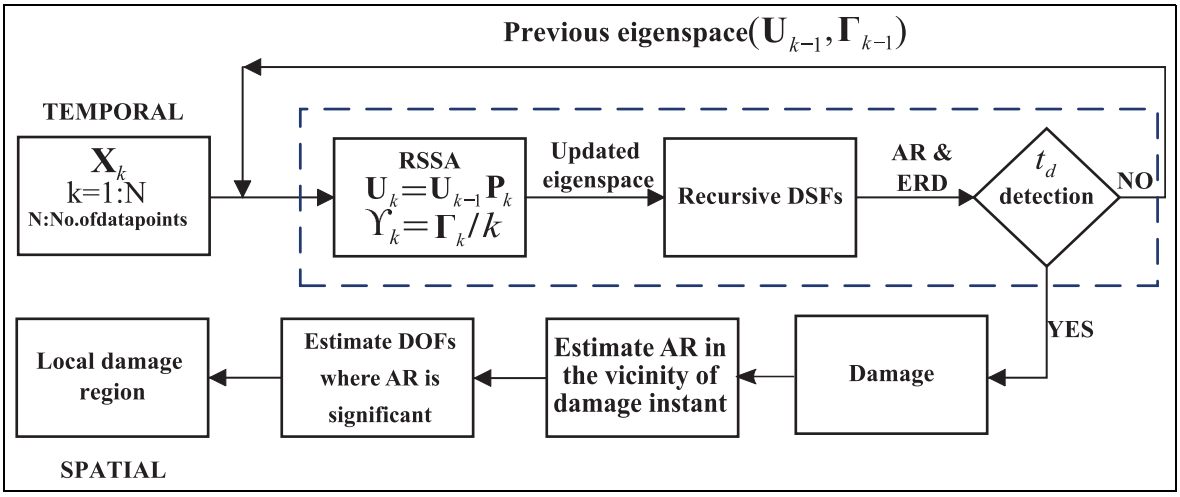

Figure 1. Basic framework of the proposed algorithm.

global damage to the structure (Figure 2). In order to quantitatively represent this damage, an empirical damage[8] is used in this study. The empirical DI is expressed as follows[8]

$$DI = 1 - \left(\frac{K_1}{K_0}\right) \tag{32}$$

where (K_1/K_0) is defined as the ratio between the secant modulus (K_1) associated with a changed level of nonlinearity (damaged state) to the initial secant modulus (K_0) of the pristine (undamaged) state. The value of the index becomes zero when the ratio (K_1/K_0) becomes unity, thereby indicating the cases of no damage to the system. The model under study has been adapted from a separate work by the authors (accepted in the *Journal of Mechanical Systems and Signal Processing*,[8] involving the use of RPCA along with TVAR in order to identify damage and its location.

Description of the single-story modeled with Duffing oscillator

The Duffing oscillator is one of the prototype systems of nonlinear dynamics. The system has been successfully used to model a variety of physical processes such as stiffening springs, beam buckling, nonlinear electronic circuit. The source of the nonlinearity in a structural system that results in its dynamic behavior being modeled by the Duffing equation is the stiffness. In this section, a simple model involving a single-story structure with a Duffing oscillator at its base is described through the following equation of motion

$$m\ddot{X} + c\dot{X} + k(X + \alpha X^3) = F(t) \tag{33}$$

The excitation $F(t)$ is zero-mean white noise with spectral density S_0. Solving the equation of motion numerically, the statistics of the response $X(t)$ can be obtained. The numerical values for system and excitation parameters are $k = 1$, $m = 1$, $c = 0.1$, $\alpha = 0.05$, and $S_0 = 1$.

Detection results using the proposed framework

Case studies are undertaken for both global and local damage using the proposed algorithm. Temporal damage detection studies are carried out by changing the value of the nonlinear force term κ at a particular instant of time. Studies for local damage detection involve the test of detection performance for the case of MDOF system subjected to progressive decrease in floor-wise stiffness at steps of 15% for each 10 s interval. This closely emulates the effects of a real-life event (such as earthquake) over a structure where the degradation occurs through stages involving sequential reduction in story stiffness (i.e. plastic hinge formation) that would ultimately lead to its collapse.

Temporal damage detection results

Case studies for 15% and 30% change in nonlinearity are provided in this section. As evident from the literature, damages of the order of 25% have been often reported as a lower limit for vibration-based damage detection.[28] However, this work successfully provides damage detection results for 15% change in nonlinearity using the real-time acceleration response from a single channel as input. Since the transformed responses obtained using the RSSA algorithm consists of simpler

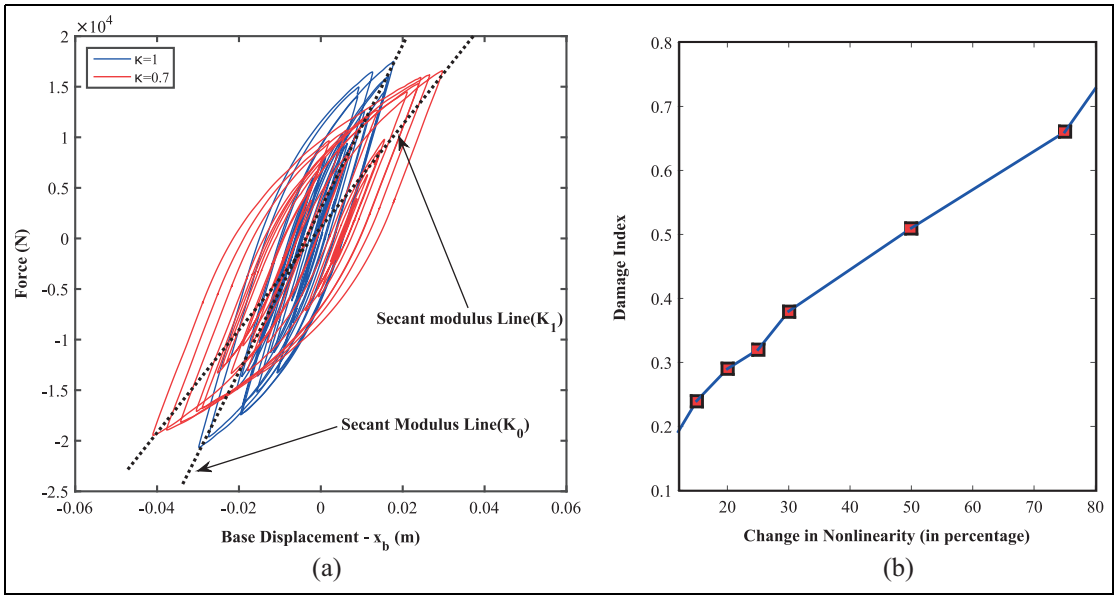

Figure 2. Force–displacement variation for various levels of nonlinearity, adapted from Krishnan et al:[28] (a) change in nonlinearity = 30% and (b) damage index for varying levels of nonlinearity.

components, a relatively low model order (which is 2 in this article) can be used. It can be observed from Figure 3 that the reduced order response obtained after the RSSA algorithm is not completely devoid of noise. The presence of both process noise and measurement noise could be discerned from the figure. In addition, the time series as well as the fast fourier transform (FFT) plots of the response shown in Figure 3 clearly indicates the presence of both process noise and measurement noise in the signal, thereby justifying the use of Kalman filter estimate in order to recursively update the algorithm at each time stamp. However, in order to recursively estimate the Kalman gain at each step more robustly, the reconstruction of the time series is carried out by incorporating PCs from the noise subspace. The damage is detected using AR coefficients and ERD as DSFs shown in Figures 4 and 5, respectively. From both the figures, a damage instant at 31 s can be easily detected using AR coefficients by observing the sudden changes of the mean level of the plot. This confirms the use of TVAR modeling toward online detection of damage in a recursive framework. To further validate the efficacy of the proposed methodology, ERD, when examined in a recursive framework, detects the instant of damage for 15% nonlinearity change at 31 s, as observed in Figure 5. While a change in the mean level of the AR plot verifies the damage instant to be at 31 s, a distinct peak shown in the recursive ERD plots indicating the exact instant of damage further reinforces the efficacy and robustness of the algorithm.

The efficacy of the DSFs for less than 15% damage is slightly questionable which indicates that the current online framework is less reliable when the extent of damage suffered is low (i.e. less than 15%). The results are therefore not reported here for brevity. In a separate work, the authors have recently investigated the prospects of real-time damage detection using RPCA in conjunction with TVAR modeling[8] and have also reported global damage detection in the order of 15%. Thus, it suffices to say that both RPCA[8,28] and RSSA algorithms are efficient in detecting low levels of damage in real time, but the performance of RSSA algorithm surpasses the performance of the RPCA algorithm as it takes the streaming data from a *single channel* as input, as compared to the RPCA algorithm, that requires *multi-channel* data as input. Therefore, the key novelty of the work arises due to the utilization of the streaming data available from a *single channel* that provides real-time damage detection. To the best of the knowledge of the authors, this has not been reported in the literature so far.

A separate case study has been carried out taking into consideration the incorporation of mean corrected covariance estimates for real-time damage detection. Although the covariance estimate for such cases differs slightly from the updates obtained for zero-mean processes, it can be observed from Figure 6 that the variation in the DSF plots is not significant. On comparing Figures 5 and 6, it is evident that the proposed algorithm could efficiently detect real-time damage for

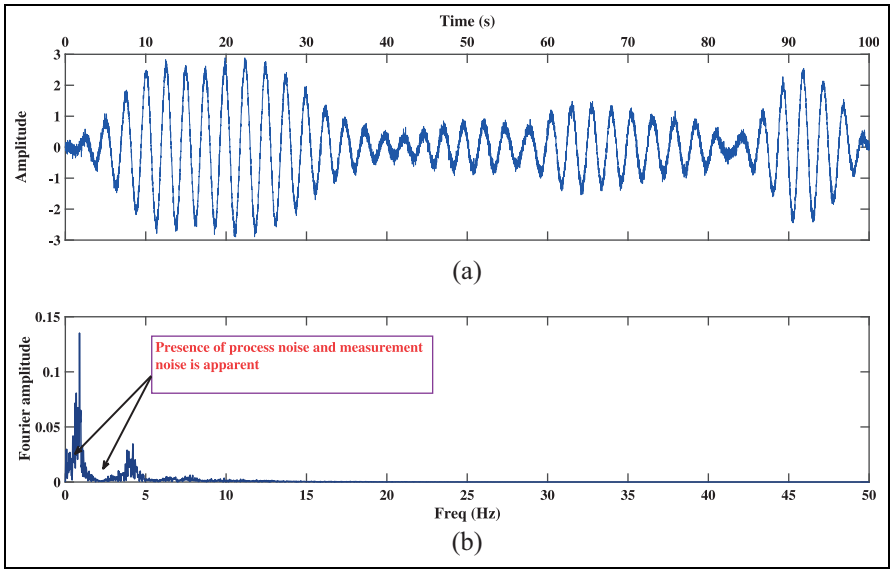

Figure 3. Plots of reduced order response and the corresponding FFT: (a) plot of reduced order response (after RSSA) and (b) FFT plot of reduced order response (after RSSA).

cases involving mean shifts as well. It can be clearly understood that the usage of $\tilde{C}$ for incorporating recursive mean estimate does not alter the detectability of the proposed algorithm significantly. For brevity, analysis for the cases involving mean shifts has been subsequently dropped for the remainder part of the manuscript.

The time taken for one complete run of the algorithm is found to 1.18 s, which approximately emulates a real-time process. The implementation of recursive eigenvalue decomposition consumes 10 ms, which is 0.85% of the total time consumed for a complete single iteration. However, the time consumed depends upon the computational power of the system used and is more efficient for systems with superior processing power, higher gigabytes of RAM, multiple cores, and so on.

Local damage detection results

In this section, the local damage detection results using the proposed algorithm are presented. The local damage is induced to the B-W model through a change in the linear story stiffness at each floor level. The salient feature developed in the local (or spatial) damage detection scheme is consistent with events where a structure undergoes varying changes in stiffness with the progression of time, for example, during an earthquake. Case studies for successive floor-wise local damage at different instants of time are provided that are validated through the use of AR plots and ERD as recursive DSFs for real-time damage detection. To this effect, the authors have carried out studies based on possible simulations closely emulating a real-life event where the stiffness of each story reduces over time.

The simulation cases considered reducing the linear stiffness of individual story by 15% at each 10-s span. Damage was numerically induced to the fifth floor at 10 s from the start, to the fourth floor at 20 s, to the third floor at 30 s, to the second floor at 40 s, and to the first floor at 50 s. The acceleration response from individual floor levels is provided as input to the algorithm to be processed in real time. The use of the same set of recursive DSFs for simultaneous global and local damage detection demonstrates the robustness of the proposed method. The results for local damage detection are presented next in detail.

The response from the fifth floor is provided as input to the algorithm and is processed by the recursive DSFs to indicate the local damage in the structure. From Figure 7, it can be seen that the change in the mean level of the AR plot occurs at 10 s, indicative of a linear stiffness change at that instant of time, for the fifth floor. On providing the acceleration response of the fourth floor as input for the algorithm, the sudden change in the mean level of the AR plot occurs at 20 s that can be interpreted as a local damage. However, an additional change in the mean level could be seen at 10 s from the start. This observation can be inferred from the fact that the fifth and the fourth floors are connected through the same column where the damage has occurred, and hence, show simultaneous peaks at both the damage instants. Similarly, the cumulative event for both the fifth and the fourth floors clearly shows that the damage has occurred to the fourth floor

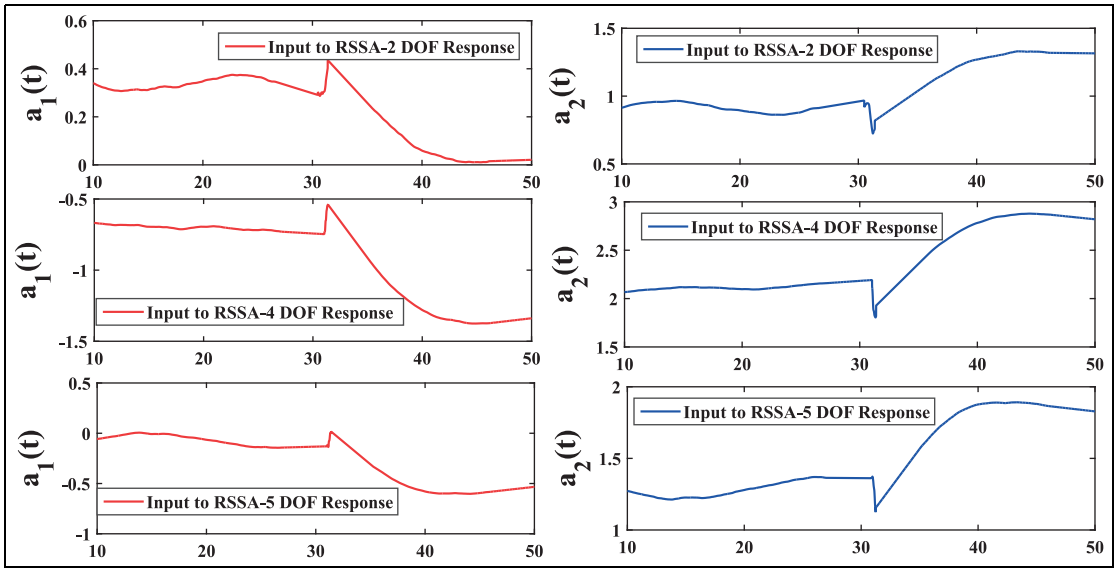

Figure 4. AR-1 and AR-2 plot for 30% global damage.

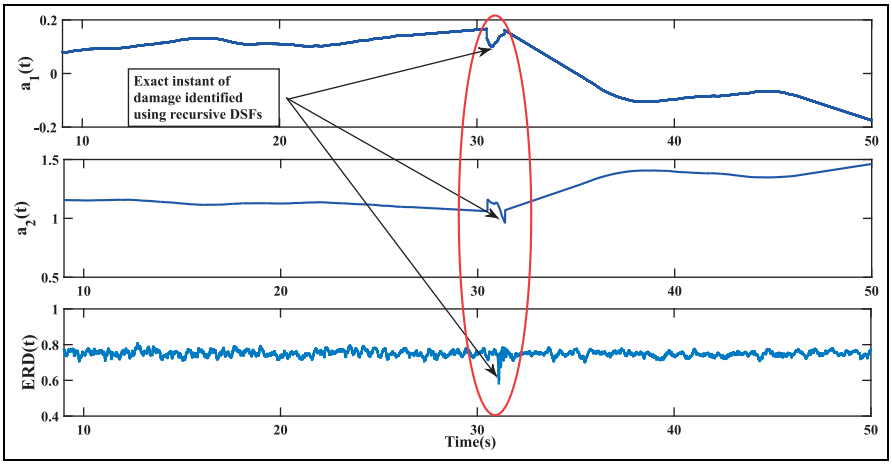

Figure 5. Recursive DSF plot for 15% global damage.

at 20 s from the start of the event. Considering the response from the third floor as input for the algorithm, two peaks are observed at 20 and 30 s, respectively, that indicate the progression of local damage in the structure, over time. Considering the cumulative event of the fifth, fourth, and the third floor, the AR plots indicate the damage to the third floor at 30 s through a change in the mean level of the plot.

The proposed algorithm is now applied on the response from the second story and is processed by the set of recursive DSFs. The change in the mean level of the AR plot occurs at 40 s from the start. As observed from the figure, the plot shows two peaks simultaneously at 30 and 40 s on considering the individual response of the second floor. However, taking into consideration the cumulative response of the fifth, fourth, third, and the second floors, the local damage at the second floor can be clearly inferred from the AR plot at 40 s. The response from the first floor when provided as input to the algorithm shows change only at 40 s from the start of the event. This result can be clearly concluded from the fact that the column connecting the second and the first floor has already suffered damage at 40 s. The cumulative event of all the floors combined indicates the damage to be at 40 s, and as the damage has stopped its progression over time, the mean level of the AR plot provides a distinctive change only at 40 s from the start. To show the efficacy of the recursive ERD in detecting the successive floor-wise local damage, the plots of ERD for

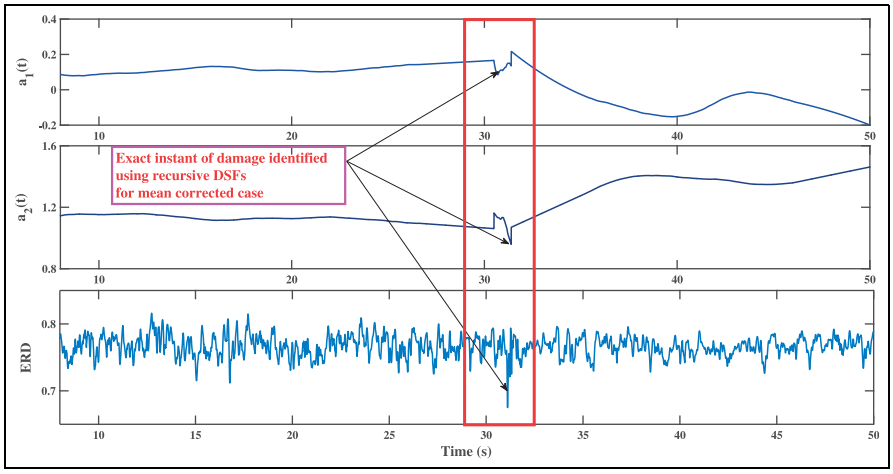

Figure 6. Mean corrected DSF plot for 15% global damage.

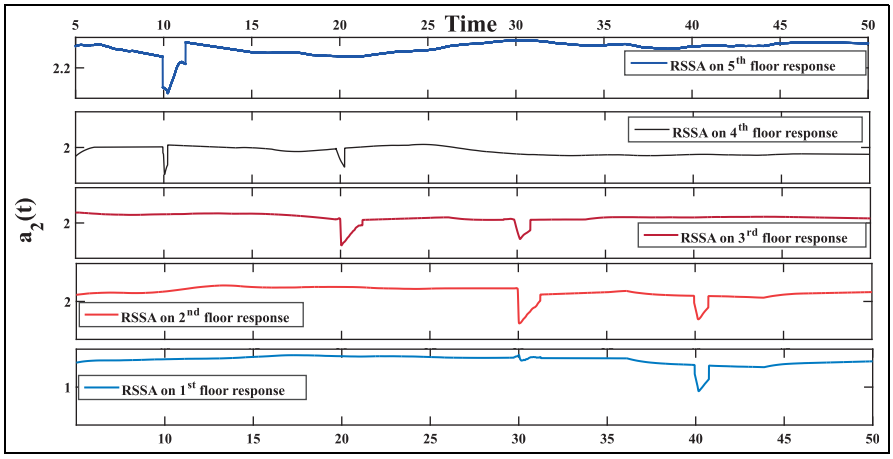

Figure 7. Local damage detection using AR coefficient—all floors.

different input cases are shown in Figure 8. It can be observed from the figure that the ERD plots behave in the same manner as the AR plots for indicating the progressive damage to the structure.

Performance of the proposed algorithm against established damage detection schemes: a comparative study

In this section, the performance of the proposed method is compared with the recently established online RPCA-based damage detection schemes. The proposed algorithm is compared against RPCA and its recursive residual error (RRE)[28] and RPCA in conjunction with TVAR modeling.[8] As the proposed damage detection method is purely *online* in nature, comparison with traditional methods such as PCA is not justified, since PCA is inherently an *offline* algorithm that requires data to be processed in batches. Windowing of the data is necessary for executing batch PCA-based damage detection which prevents any possibility of online implementation of the method. A crucial point of contrast of the proposed method with the established detection methods is the use of a *single sensor* data as input for damage detection process. RPCA-based detection schemes use a minimum of two sensors as inputs for proper functioning of the algorithm. In addition, RPCA involves updating of the covariance matrix of the data set at each time stamp, contrary to the functioning of the RSSA algorithm where the covariance update of the Hankel matrix takes place at each instant of time.

In the present context, the comparative study is conducted on the B-W model described in section "Description of the five-story structure with B-W

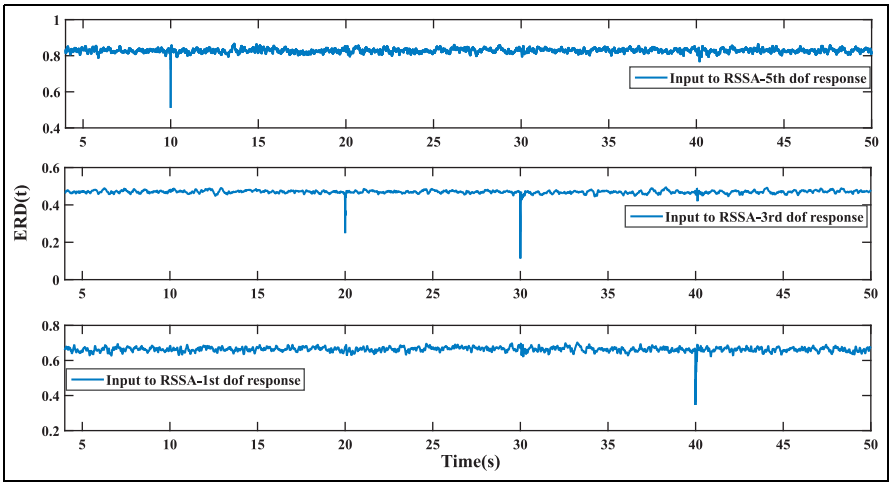

Figure 8. Local damage detection using ERD.

isolator at its base" under a white noise excitation of 50 s duration. On excitation, the third floor of the model undergoes a change in the linear stiffness by 15% at 31 s. The basis of comparison of the algorithms is to detect the change in the spatial orientation of the system in real time. As evident from the literature,[8] the damage detection potential of the RPCA algorithm is confined to the order of 25% for spatial damage. Figure 9 clearly indicates that the efficacy of both RPCA-RRE and RPCA-TVAR algorithms is slightly questionable for 15% spatial damage. While the RRE and AR plots for both the RPCA-based detection algorithms fail to show any detectable change in the mean level of the plots, the proposed RSSA algorithm captures the exact instant of damage at 31 s for a 15% linear local story stiffness change. This confirms the superiority of the proposed algorithm over the established damage detection schemes. In line with the above findings, a tabular comparison of the algorithms toward percentage change in linear story stiffness (termed as spatial damage) is provided in Table 1. It can therefore be concluded that the proposed RSSA algorithm is advantageous over RPCA-based damage detection methods in terms of an improved detectability of spatial damage in real time.

RMSSA results

In this section, the results showing the applicability of RMSSA toward the proposed B-W model are presented. RMSSA, an extension of the RSSA (or even the traditional SSA) approach, is effective in analyzing inputs from two or more channels from a system. The method is receptive toward temporal damage and indicates the exact instant of damage through a linear change in stiffness. At a particular instant of time, the linear stiffness of the third story is reduced by 30%. As the third column is affected, the neighboring DOFs are expected to show distortions as discussed in section "Local damage detection results" (kindly refer Figure 7 for further details). Since the RMSSA algorithm uses multi-channel floor response as inputs at the *same time*, it cannot be used for localization of the damage that is confined only to a single story as demonstrated in section "Local damage detection results" using multiple applications of single-channel RSSA, which clearly has an advantage over the RMSSA approach for detecting local damage. Therefore, only the temporal damage detection is demonstrated in this section using RMSSA.

To this effect, response obtained from the second and fourth floor are provided as inputs to the RMSSA algorithm. The initial signal length is selected as 6. The data processed after RMSSA is fit with TVAR models to be tracked in real time. Figure 10 provides clear detection results for a damage occurring at 31 s through deviations in the AR plots. To further substantiate the instant of damage provided by the AR coefficients, ERD is applied over the processed data and tracked in real time, as discussed in the preceding sections.

From Figure 10(a) and (b), it can be observed that the AR plots show changes in the mean level at 31 s, precisely indicating the instant of damage. Additionally, the ERD plot (Figure 10(c)) further validates the instant of damage to be the same as that observed from the AR plots. Thus, based on the above result, it is safe to interpret that RMSSA is consistent with RSSA toward an online implementation. The DSFs developed for the RSSA algorithm are amenable

Table 1. Comparison of existing damage detection methods with the proposed algorithm.

Local damage (%)	RPCA-RRE	RPCA-TVAR	Proposed algorithm
35.00	Yes	Yes	Yes
25.00	Yes	Yes	Yes
20.00	No	Yes	Yes
15.00	No	No	Yes

RPCA: recursive principal component analysis; RRE: recursive residual error; TVAR: time-varying autoregressive.

Results for the SDOF Duffing oscillator model

The results for damage detection of the one-DOF oscillator model using the proposed algorithm are presented in this section. In this approach, the acceleration response from the model is provided as input to the algorithm and is processed online to indicate damage through the DSFs. The damage is induced through a change in the α parameter as shown in equation (33). The change in the parameter α is analogous to a change in the value of κ (equation (30)) that indicates an alteration in the nonlinear force term. Similar to the B-W model, the single story modeled with the Duffing oscillator also undergoes a global damage when the force

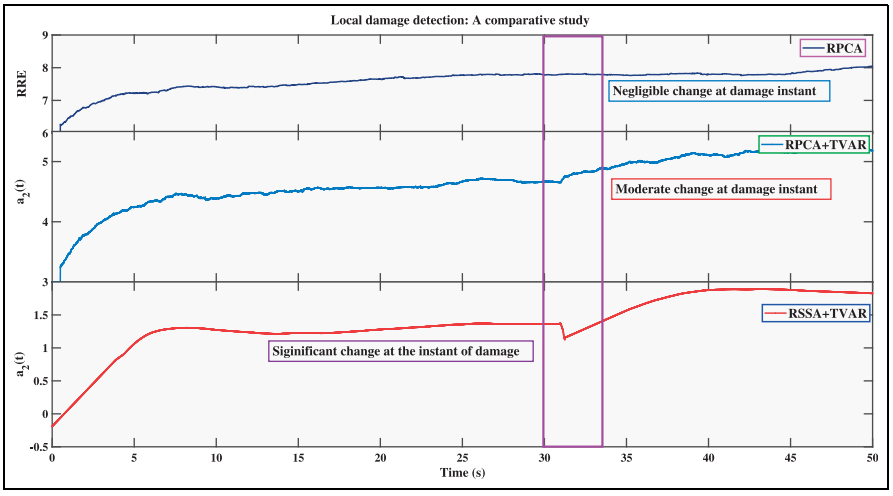

Figure 9. Comparison of the recently established damage detection methods with the proposed algorithm.

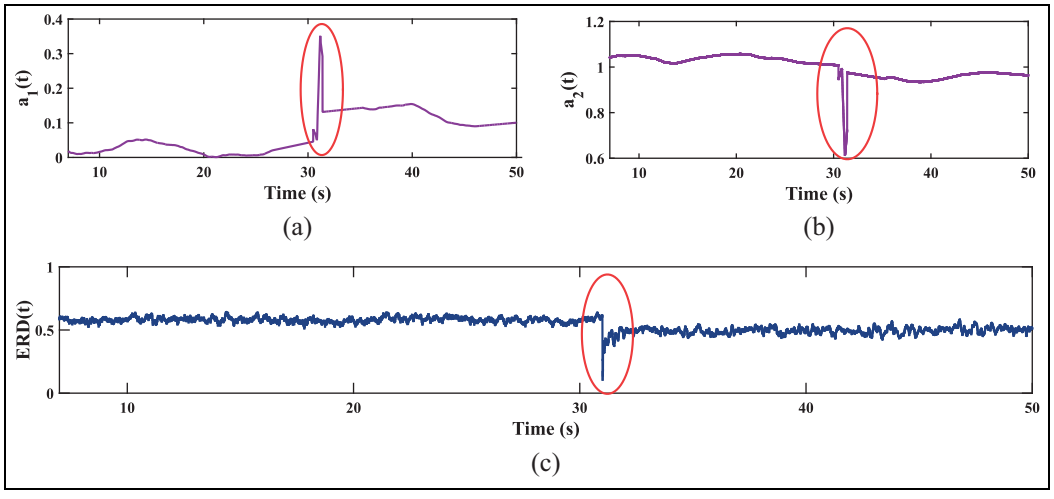

Figure 10. Detection results using RMSSA: (a) AR-1, (b) AR-2, and (c) ERD.

toward damage detection for RMSSA as well, showing good detection results for multi-channel inputs developed toward this study.

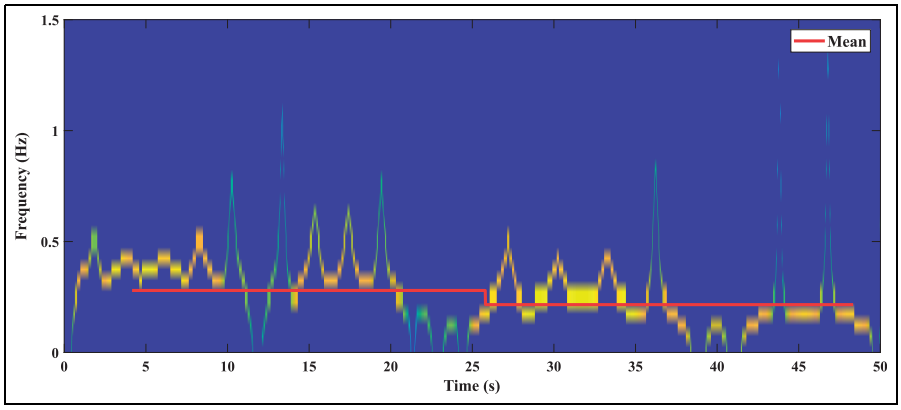

Figure 11. Hilbert–Huang spectrum for SDOF Duffing oscillator.

parameter controlling the effect of nonlinearity is changed at a particular instant of time. The damage is induced to the model at 26 s from the start, through a 25% change in the nonlinear force term of equation (33).

A plot of Hilbert–Huang spectrum (HHS) for the SDOF Duffing oscillator is shown in Figure 11. Empirical mode decomposition (EMD) applied to the acceleration response yields intrinsic mode functions (IMFs)[43–45] for application of Hilbert spectral analysis. Although plots of both FFT and HHS are approximate spectral representations of a signal evolving from a nonlinear system, the use of HHS to study nonlinear systems and signals is well documented in the literature.[43,45] Therefore, spectral representations of nonlinear systems are studied through HHS plots in the draft. In the present context, IMFs having significant energy content were chosen for the subsequent plotting of the HHS. The mean frequency is calculated on the basis of the average of the frequencies obtained from the instantaneous values of the Hilbert phase, considered event to event in time. Figure 11 shows the variation in the mean frequency content of the system which roughly corroborates to the changes in the system occurring due to a possible damage at a certain instant of time. A noticeable feature of the HHS is the change in the mean level of the frequency band only at 26 s, thereby, indicating the possible event at 26 s. However, it should be noted that the purpose of these plots is purely to serve as a visual aid for identifying the instant of damage and does not play any role in the real-time functioning of the algorithm. Using the proposed algorithm, the detection results for the Duffing oscillator is shown in Figure 12. It can be observed from the figure that the plots of AR-1 and AR-2 clearly indicate an accurate damage instant at 26 s. Figure 12(a) and (b) shows a discernible change in the mean level of the AR plots at the instant of damage. A change in the mean plot verifies the efficacy of the DSF to detect damage even for a single-story structure with a nonlinear parameter associated with it. Based on these interpretations, it becomes very clear to explain the sudden change in the mean level of the ERD plot shown in Figure 12(c). As clearly validated from the ERD plot, the exact instant of damage indeed occurs at 26 s. The detection results provided in this section substantiates the use of the proposed methodology towards identifying global damage for a varied category of nonlinearities associated with systems.

Experimental verifications

Experimental studies were conducted in a laboratory environment to verify the applicability of the proposed algorithm toward solving real-time damage detection problem. To substantiate the robustness of the proposed algorithm, two case studies have been presented:

1. An experimental model setup in a laboratory environment comprising of an aluminum beam excited by a ground motion, having a rubber strip attached to its free end.
2. A SDOF system modeled as a cart attached to springs on either side of the mass experimented with a Gaussian white noise to detect damage through a change in the stiffness of the system.

Aluminum beam experiment

An experimental setup has been devised to emulate an online damage and the current algorithm has been utilized to identify the instant of damage in real time (Figure 13). The setup consists of an aluminum beam of dimension 120 cm×3.5 cm×0.5 cm fixed on a base plate, drilled on top of a shake table (model no. Bi-00-

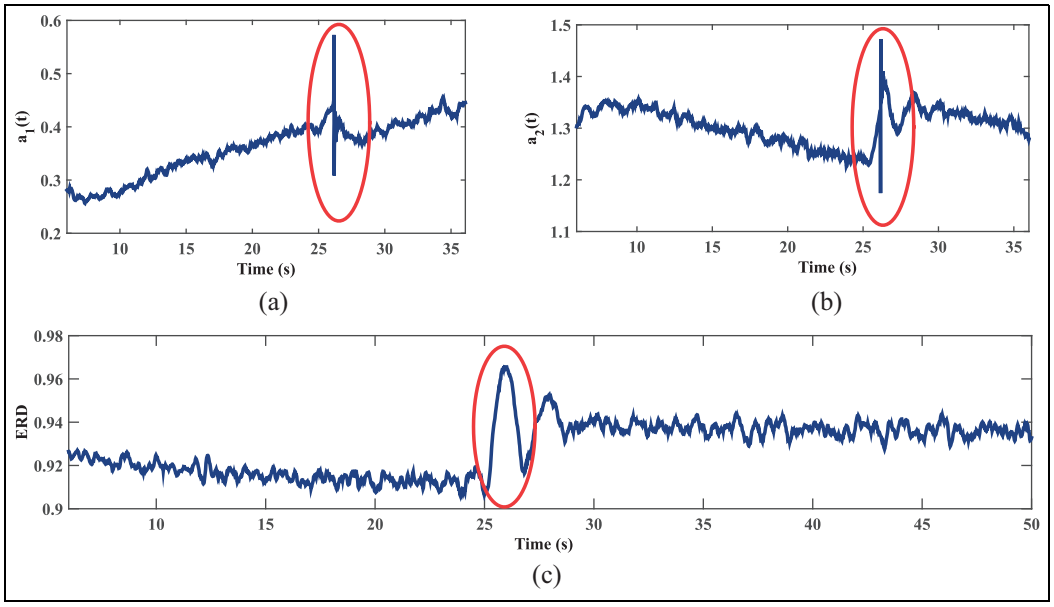

Figure 12. Damage detection for SDOF Duffing oscillator: (a) AR-1, (b) AR-2, and (c) ERD plot.

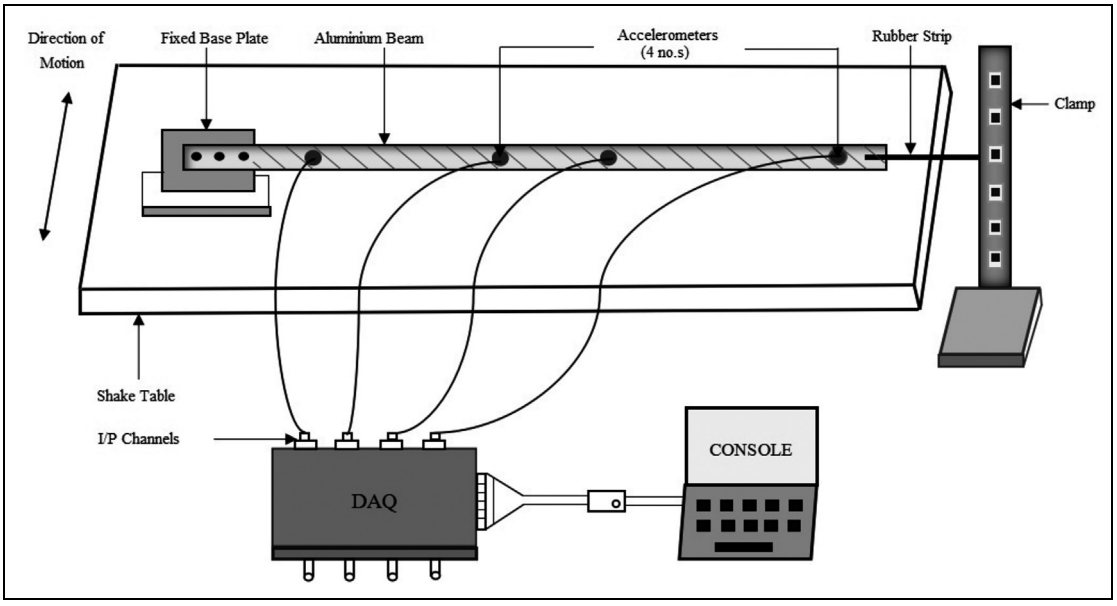

Figure 13. Details of the experimental setup.[28]

300). The base plate is a welded structure of two plates at a right-angle butt weld bearing dimensions of 23 cm×15 cm×1 cm each. The shake table is specified as (1) table dimensions—150 cm×150 cm; (2) payload capacity—5 ton; (3) peak velocity—153 cm/s; (4) peak acceleration—±2.0 g; (5) frequency range—0–20 Hz. The model is subjected to an earthquake excitation and the acceleration data are collected using QuantumX MX410 HBM Data Acquisition System (DAQ) at a sampling frequency of 75 Hz. The aluminum beam model is instrumented using Honeywell accelerometers TEDS by HBM at four positions. The positions of the four accelerometers from the free end are 1, 30, 47, and 81 cm, respectively. The free end of the cantilever beam is attached with a thin rubber strip (Figure 13) which has a taut length of 70 cm and the other end of which is clamped rigidly on a heavy steel platform. This rubber strip induces a nonlinearity to the experimental

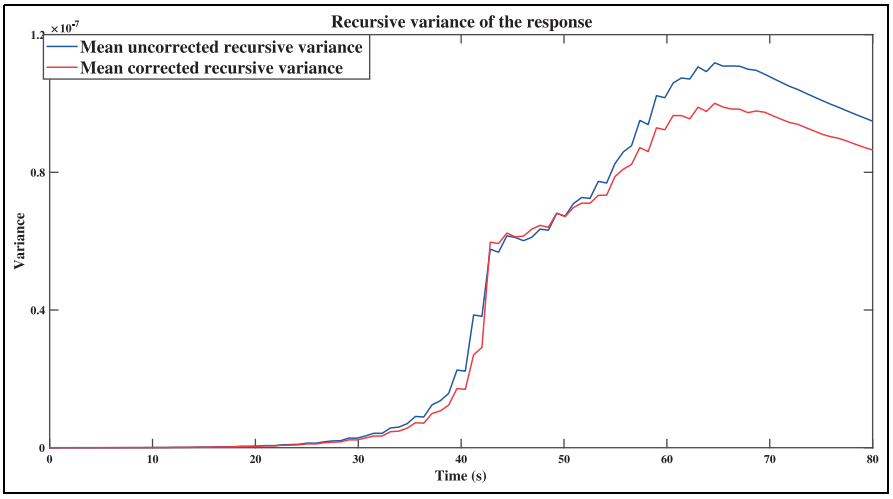

Figure 14. Recursive statistics of the response.

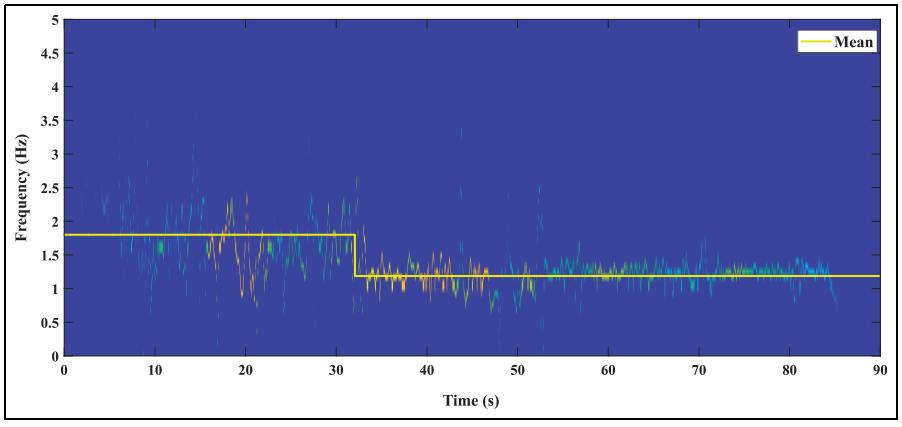

Figure 15. Hilbert–Huang spectrum for the aluminum beam experiment.

setup. This model can be readily used to validate the accuracy of the proposed method as explained in the following segment.

The experiment is carried out by subjecting the aluminum beam to a scaled ground motion (1999 Chi-Chi ground motion, scaled to peak 0.3*g*). In order to simulate a real-time damage scenario, the rubber strip attached to the free end of the cantilever beam is snapped accurately at a fixed time instant, during the shaking motion of the beam. The measurement of the instant of the snap is done using a stop watch and the entire experiment is recorded in the form of videos to ensure accurate measurement of the instant. Although damage ideally should be an instantaneous phenomenon, the action of snapping as observed after repeated trials of experimentation takes at least 0.5–1 s. This small lag should be considered while calculating the damage instant. Hence, it is safe to assume that there is a possibility of a practical error of 0.5–1 s in recording the time of damage. Thus, the recorded time of damage should be considered as 33 ± 1 s. The applicability of the proposed method for cases involving nonstationary data could be well understood from Figure 14. It is evident from the figure that the response is clearly nonstationary, as evident from the evolution of the recursive variance. Furthermore, it should be noted that the mean corrected and the mean uncorrected recursive variance of the response are approximately similar. The potential of the proposed method to detect damage for cases involving nonstationary nature of the input data is discussed next.

In order to represent the phenomena of damage for the experiment, the HHS for the present case is shown in Figure 15. As seen from the figure, a damage at 33 s can be approximately inferred through a change in the mean level of the frequency content of the instantaneous phase. Out of the four IMFs obtained from EMD, the fourth IMF having significant energy content was used for the calculation of the HHS. As the occurrence of some background noise during the trials of the experiment is inevitable, the HHS serves as an approximate visual aid for the detection of the damage

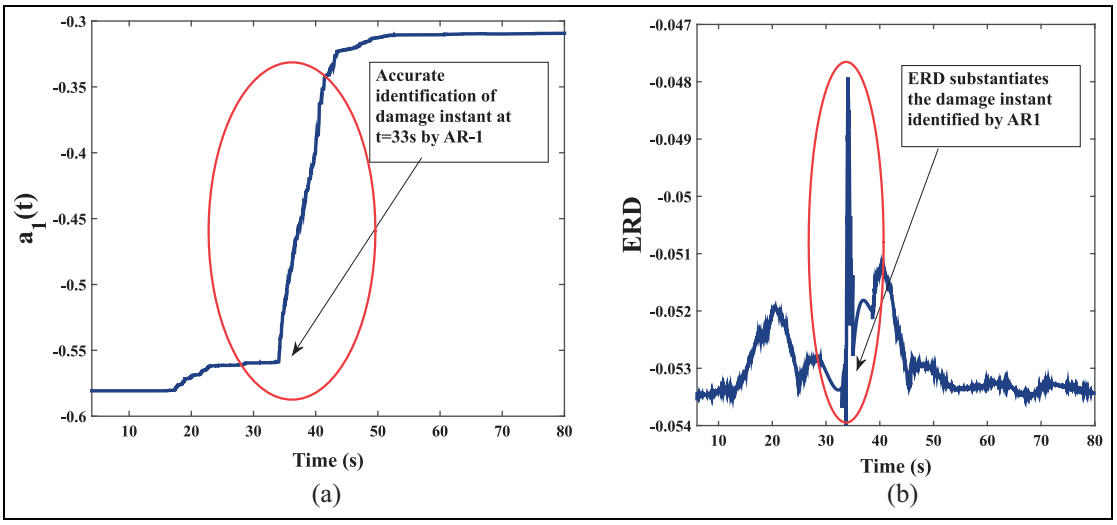

Figure 16. DSFs for the aluminum beam experiment: (a) AR-1 and (b) ERD.

instant when supplemented with the mean frequency line. In line with most of the literature relating frequency shifts as indicators of damage,[45] Figure 15 provides a reasonable first-hand representation of the damage scenario for the experimental case. As mentioned earlier, it should be noted that the implementation of these plots is purely offline in nature and are useful in providing approximate visual aids toward ascertaining damage. To further confirm the presence of damage, the data are processed through the proposed RSSA-based real-time damage detection algorithm which is discussed next.

The proposed algorithm is applied on the raw acceleration data streaming in real time, acquired by the QuantumX DAQ. It can be observed from Figure 16 that TVAR coefficient $a_1(t)$ shows a significant change in mean level of the plot at 33 s and persists with the same mean level till the end of the acquisition (experiment). This indicates the occurrence of damage at 33 s which is further validated by the use of ERD (Figure 16(b)) estimated in a recursive fashion over the data set processed by the RSSA algorithm. As observed in Figure 16(b), the peak at 33 s clearly indicates the instant of damage. Thus, it is safe to conclude that the proposed method is effective in identifying the instant of damage in real time under experimental conditions.

Toy cart experiment

Figure 17 shows the setup consisting of an SDOF system which is physically modeled as 100 g mass cart attached with three springs on either side whose other end is connected to fixed supports. The combined stiffness of the attached spring assembly is calculated as 0.379 N/mm. The whole setup is arranged on top of a

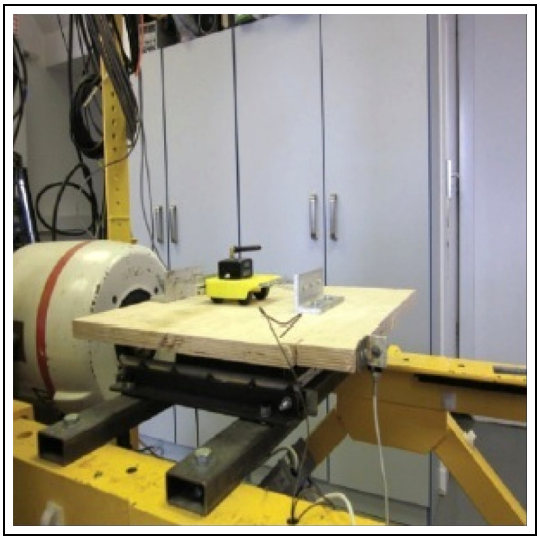

Figure 17. Setup for the toy cart experiment (adapted from Pakrashi et al.[46]).

vibration bench which is excited by an input force of suitable intensity. The structural damping is usually considerably below critical damping and the system undergoes forced vibration. While assuming the damping of the simulated model, free vibration decay of the physically built model was considered and an estimated value of 2% equivalent viscous damping ratio was used. Accelerometers placed on top of the vibration bench and the mass cart measured the input acceleration and the output response data, respectively, at a sampling rate of 830 Hz. In order to ensure the accuracy of the measured data, laser doppler vibrometer (LDV) attached to the cart measured the velocity of

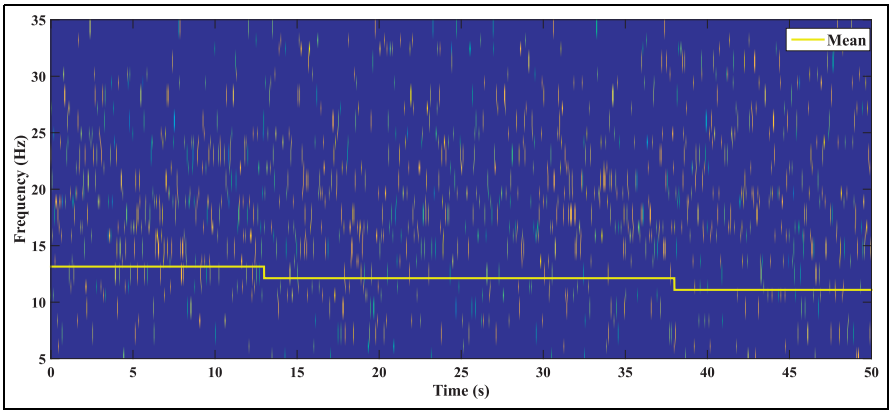

Figure 18. Hilbert–Huang spectrum for the toy cart experiment.

motion at a sampling rate of 128 Hz, to obtain the output acceleration data through integration. Although the springs are linearly calibrated in tension under static loading and to a certain displacement, the combined system is not guaranteed to exhibit linear model behavior as obtained from linear or weakly nonlinear simulations.

The experiment is carried out by subjecting the vibration bench to a Gaussian white noise excitation and the response data sampled at a prefixed frequency. During the vibrational motion of the mass cart, the springs are carefully sheared at a particular time instant, in order to simulate a real-time damage scenario.[46] In the present study, two damage instances are created by shearing two different springs at different time instants. The first damage instant, at $t = 13$ s, reduces the overall stiffness from 0.378 to 0.303 N/mm (stiffness reduction of around 19%). The second break induces a stiffness alteration of around 17%, by reducing the equivalent stiffness from 0.303 to 0.249 N/mm at $t = 38$ s.[46]

A plot of HHS showing the time-varying instantaneous frequencies and the changes in the average frequency line is presented in Figure 18. The change in the average frequency is represented by the yellow line which estimates the average of the instantaneous frequencies considered event wise (i.e. from the beginning to the first shearing, first shearing to the next shearing). On applying EMD on the acceleration responses, IMFs were generated. The first four IMFs corresponding to the maximum energy content were used for representing the HHS. Figure 18 shows changes in the mean level of the frequency in three stages, indicating the exact instant of shearing of the springs. Furthermore, it can be observed from the mean frequency line that there is a change in 13 s that continues at a steady magnitude until the point of next shearing. A change in the mean level at 38 s approximately indicates a possible event for the experiment. The mean values of the frequency obtained from the HHS plot for the toy cart experiment case are found to be 13.15, 12.12, and 11.09 Hz. The corresponding percentage changes in the frequencies are calculated to be 7.8% for the first shear and 8.5% for the second shear, respectively, that conforms to the traditional notion of damage in the system. However, the presence of background noise makes it difficult to discern the changes in the instantaneous frequencies themselves (without the mean frequency line), thereby rendering the visual interpretation of the HHS, difficult. To further confirm these approximate findings, detailed analysis using the proposed RSSA-based framework is considered next.

The raw vibration data streaming from the accelerometer and LDV are accurately recorded at a fixed sampling rate using suitable DAQ. The proposed algorithm is applied to the acceleration data in order to identify the exact instant of damage. The damage instant is accurately identified by the DSF as observed from Figure 19. It is clear from the figure that TVAR coefficients $a_1(t)$ and $a_2(t)$ both show changes in the mean level at the instants of damages (13 and 38 s, respectively). The proposed experimental verification further validates the sensitivity of the current framework to detect structural damages as low as 17%, for a practical scenario. As clearly observed from Figure 19(a) and (b), TVAR coefficients provide good indicators of damage for the observed damage cases. It should be noted that although the presence of noise during an experiment is inevitable, the algorithm still detects the damage instants to a fairly good level of accuracy. The successive instants of damage are efficiently captured by the recursive coefficients, indicating that the algorithm works well even for cases with multiple damages.

It should be noted that for slowly decaying mechanisms such as corrosion, the impact of the embedded variables plays a significant role in determining the accurate instant of damage, leading to a mixing of the

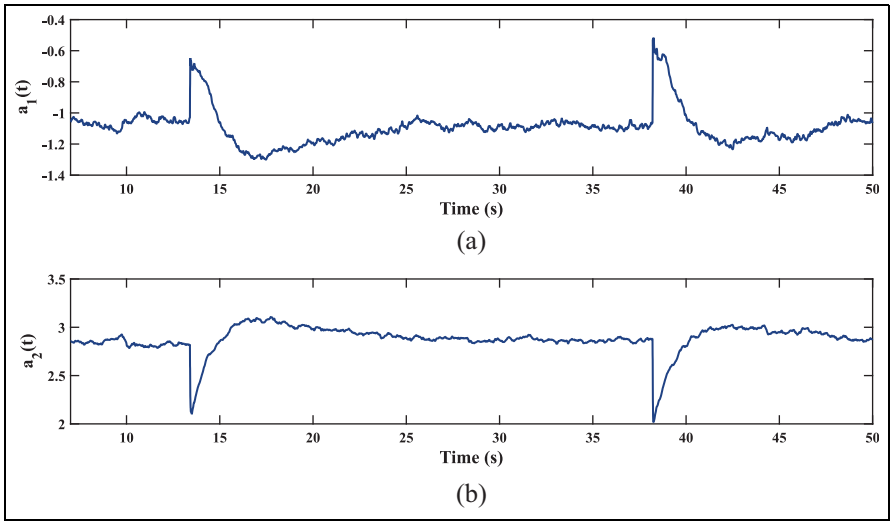

Figure 19. DSFs for the toy cart experiment: (a) AR-1 and (b) AR-2.

original and the newer states. The embedded variables need to be processed in batches. The difficulty in measuring the real-time changes in environmental and operational conditions (such as temperature, humidity, wind) arises due to cost factors, complexity in determining the optimal locations of sensors, and susceptibility toward false detections. These slow varying processes might hinder the applicability of the proposed algorithm toward real-time implementation and might lead to the masking of environmental variations. The potential implementations of the proposed algorithm range from real-time damage detection of civil structures, to data-driven mechanical and aerospace applications where the acquisition of time series data is possible. Multiple real-life possibilities range from fault detection of gear boxes, detection of cracks in airplane to nonlinear damage detection in structures, instrumented with either a single sensor or even a dense array of sensors located at strategic points for health monitoring. The proposed algorithm shows effective results even for multi-channel inputs, in a recursive framework, closely emulating real-life instances where the structures are subjected to low levels of damage due to external excitations.

Case study for UCLA Factor Building: a practical problem involving large data dimension

The applicability of the proposed algorithm toward large data dimension is an important aspect to ensure the robustness of the algorithm toward practical problems as well. The proposed method is now applied to the vibration data collected from the Doris and Louis Factor Building (UCLAFB), which is a major G + 15 story, 216.5 ft high[8,15,28] facility located in the University of California campus in Los Angeles (UCLA). The building was instrumented with a dense array of 72 Kinemetrics FB-11 uniaxial accelerometers at all the floor levels. Each level has two pairs of orthogonal sensors parallel to the N-S and E-W directions. The array of sensors is converted to an equivalent array of N-S, E-W, and θ directional sensors lumped at the center of rigidity of each of the floors.[15] This building is permanently instrumented, and the vibration data from this building are made available for researchers world-wide through a remote database server. The data are sampled at 100 Hz. In order to examine the efficacy and damage detection potential of the proposed algorithm, floor accelerations due to the combined ambient data and earthquake data response (with Mw = 6.0, on 28 September 2004, 10:15 AM pacific daylight time from Parkfield, CA) are considered.

UCLAFB has been studied extensively in recent times mostly in the context of output only modal identification and the results are reported in some published works.[8,15,28] Vibration response obtained from the database server suggests that a considerable incidence of nonstationary activity in the vicinity of $t = 360$ s indicates the onset of the Parkfield earthquake. Out of the 48 responses obtained from the data set, the translational responses are utilized for online processing using the proposed algorithm. The acceleration response of the roof and third floor for the E-W component are considered for a close analysis through the proposed RSSA-based algorithm.

It is evident from Figure 20 that the change in the mean level of the AR plot for both the floor responses around $t = 360$ s indicates the onset of the earthquake

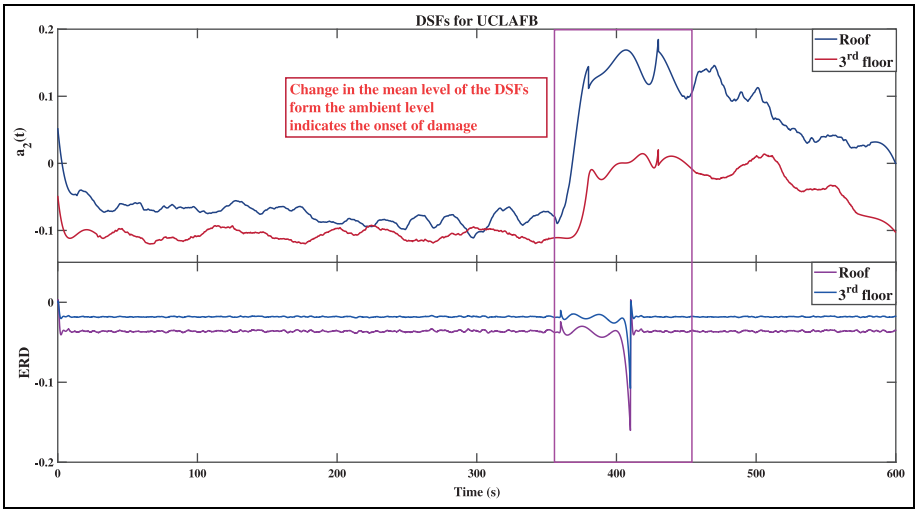

Figure 20. DSFs for the UCLAFB.

that continues up to $t = 410$ s, indicative of pronounced structural damage. It is normal to expect these two instants to be different from each other because it takes a finite time for the structure to undergo significant changes, reflected through a change in stiffness. Previous modal identification studies on UCLAFB[15] provide 14.31%, 13.95%, 15.61%, 8.49%, 7.24%, 4.95%, 4.95%, 30%, 6.5%, 4.75% reduction in the values of identified frequencies between ambient vibration and earthquake data, which indicates significant global reduction in stiffness values. In addition to the AR plots, ERD plots (Figure 20) when examined in a recursive framework, show deviation from the ambient regime at around $t = 360$ s and significantly in the vicinity of $t = 410$ s indicating the occurrence of damage. Hence, it can be concluded that the proposed algorithm could be extensively used for damage detection of real-life structures involving large data dimension under nonstationary cases as well.

Conclusion

A real-time damage detection algorithm for vibrating systems based on RSSA in conjunction with TVAR model is presented. Recursive updates of the eigen subspace using rank-one perturbation facilitated real-time evolution of the PCs, eliciting the maximum information contained for damage detection. Subsequent modeling of PCs explaining maximum variance makes the transformed response amenable to a low order TVAR model which is a key step of the proposed framework. The use of AR coefficients as viable DSFs facilitated real-time temporal damage detection for the system. The potential of ERD toward an online implementation provided substantial evidence to validate the damage instants detected through the use of AR coefficients, pitched in a recursive framework. The proposed framework provided successful detection results for damages even up to 15% for the white noise excitation and up to 17% stiffness reduction for the experimental case. RMSSA provides good detection results up to 30% linear stiffness change for a particular story. The proposed method shows accurate damage instants through changes in the mean level of the plots for numerically simulated systems. Case studies show that the algorithm is equally capable of detecting damage online through experimental setups based on global damage schemes. The superiority of the RSSA-based framework over its traditional offline version shows promising potential from a real-time damage detection standpoint. The presented case studies provide evidence that the algorithm could suitably be used for real-life scenarios even for single-channel inputs, which is sometimes the case, considering cost and other factors. The proposed method detects damage in a recursive framework for multi-channel inputs using the same set of DSFs developed for RSSA, thereby reducing computational exhaustion and extending its applicability toward a diverse range of damage detection problems. Global damage detection problems for different categories of nonlinearities associated with a system is kept as an extension of the current work to be dealt with in the future.

Authors' Note

Manu Krishnan is now affiliated to Department of Aerospace and Ocean Engineering, Virginia Tech, Blacksburg, USA.

Declaration of conflicting interests

The author(s) declared no potential conflicts of interest with respect to the research, authorship, and/or publication of this article.

Funding

The author(s) received no financial support for the research, authorship, and/or publication of this article.

References

1. Znidaric A, Pakrashi V, O'Brien EJ, et al. A review of road structure data in six European countries. *J Urban Design Plan* 2011; 164(4): 225–232.
2. Farrar CR and Worden K. An introduction to structural health monitoring. *Phil Trans Royal Soc Lon A* 2007; 365(1851): 303–315.
3. Balageas D, Fritzen C-P and Güemes A. *Structural health monitoring*, vol. 493. Hoboken, NJ: John Wiley & Sons, 2006.
4. Farrar CR and Worden K. *Structural health monitoring: A machine learning perspective*. Hoboken, NJ: John Wiley & Sons, 2012.
5. Doebling SW, Farrar CR, Prime MB, et al. A summary review of vibration-based damage identification methods. *Shock Vibrat Dig* 1998; 30(2): 91–105.
6. Yan YJ, Cheng L, Wu ZY, et al. Development in vibration-based structural damage detection technique. *Mech Syst Sig Proc* 2007; 21(5): 2198–2211.
7. Sadhu A and Hazra B. A novel damage detection algorithm using time-series analysis-based blind source separation. *Shock Vibrat* 2013; 20(3): 423–438.
8. Krishnan M, Bhowmik B, Hazra B, et al. Real time damage detection using recursive principal components and time varying auto-regressive modeling. *Mech Syst Sig Proc* 2017; 101: 549–574.
9. Nair KK, Kiremidjian AS and Law KH. Time series-based damage detection and localization algorithm with application to the ASCE benchmark structure. *J Sound Vibrat* 2006; 291(1): 349–368.
10. Dackermann U, Smith WA and Randall RB. Damage identification based on response-only measurements using cepstrum analysis and artificial neural networks. *Struct Health Monitor* 2014; 13(4): 430–444.
11. Curadelli RO, Riera JD, Ambrosini D, et al. Damage detection by means of structural damping identification. *Eng Structures* 2008; 30(12): 3497–3504.
12. Pandey AK, Biswas M and Samman MM. Damage detection from changes in curvature mode shapes. *J Sound Vibrat* 1991; 145(2): 321–332.
13. Yan AM, Kerschen G, De Boe P, et al. Structural damage diagnosis under varying environmental conditions—part I: a linear analysis. *Mech Syst Sig Proc* 2005; 19(4): 847–864.
14. Merz B, Kreibich H, Thieken A, et al. Estimation uncertainty of direct monetary flood damage to buildings. *Nat Hazard Earth Syst Sci* 2004; 4(1): 153–163.
15. Hazra B and Narasimhan S. Wavelet-based blind identification of the UCLA Factor building using ambient and earthquake responses. *Smart Mater Struct* 2010; 19(2): 025005.
16. Behmanesh I and Moaveni B. Probabilistic identification of simulated damage on the Dowling Hall footbridge through Bayesian finite element model updating. *Struct Control Hlth* 2015; 22(3): 463–483.
17. Brownjohn JMW, Xia P-Q, Hao H, et al. Civil structure condition assessment by FE model updating: methodology and case studies. *Finite Element Analys Design* 2001; 37(1): 761–775.
18. Mottershead JE and Friswell MI. Model updating in structural dynamics: a survey. *J Sound Vibrat* 1993; 167(2): 347–375.
19. Skolnik D, Lei Y, Yu E, et al. Identification, model updating, and response prediction of an instrumented 15-story steel-frame building. *Earthquake Spectra* 2006; 22(3): 781–802.
20. Carden EP and Fanning P. Vibration based condition monitoring: a review. *Struct Health Monitor* 2004; 3(4): 355–377.
21. Fan W and Qiao P. Vibration-based damage identification methods: a review and comparative study. *Struct Health Monitor* 2011; 10(1): 83–111.
22. Li YY and Chen Y. A review on recent development of vibration-based structural robust damage detection. *Struct Eng Mech* 2013; 45(2): 159–168.
23. Misra M, Yue HH, Qin SJ, et al. Multivariate process monitoring and fault diagnosis by multi-scale PCA. *Comput Chem Eng* 2002; 26(9): 1281–1293.
24. Hassani H. A brief introduction to singular spectrum analysis. *Optim Decis Statis Data Anal* 2010; 13, www.ssa. cf. ac. uk/a_brief_introduction_to_ssa. pdf.
25. Golyandina N and Zhigljavsky A. Singular spectrum analysis for time series. *Earth Eng Struct Dynam* 2013; 44(6): 831–848.
26. Elsner JB and Tsonis AA. *Singular spectrum analysis: A new tool in time series analysis*. London: Springer Science & Business Media, 2013.
27. Yu L, Zhu JH and Yu LL. Structural damage detection in a truss bridge model using fuzzy clustering and measured FRF data reduced by principal component projection. *Adv Struct Eng* 2013; 16(1): 207–217.
28. Krishnan M, Bhowmik B, Tiwari AK, et al. Online damage detection using recursive principal component analysis and recursive condition indicators. *Smart Mater Struct* 2017; 26(8): 085017.
29. Liu K, Law SS, Xia Y, et al. Singular spectrum analysis for enhancing the sensitivity in structural damage detection. *J Sound Vibrat* 2014; 333(2): 392–417.
30. Hassani H, Xu Z and Zhigljavsky A. Singular spectrum analysis based on the perturbation theory. *Nonlinear Anal* 2013; 12(5): 2752–2766.
31. Chao SH and Loh CH. Application of singular spectrum analysis to structural monitoring and damage diagnosis of bridges. *Struc Infrastruct Eng* 2014; 10(6): 708–727.

32. Lakshmi K, Rao A and Gopalakrishnan N. Singular spectrum analysis combined with ARMAX model for structural damage detection. *Struct Control Hlth* 2016; 24(9): e1960.
33. Li W, Yue HH, Valle-Cervantes S, et al. Recursive PCA for adaptive process monitoring. *J Proc Control* 2000; 10(5): 471–486.
34. Golub GH and Van Loan CF. *Matrix computations*, vol.3. Baltimore, MD: JHU Press, 2012.
35. Gul M and Catbas FN. Statistical pattern recognition for structural health monitoring using time series modeling: theory and experimental verifications. *Mech Syst Sig Proc* 2009; 23(7): 2192–2204.
36. Hazra B, Sadhu A and Narasimhan S. Fault detection of gearboxes using synchro-squeezing transform. *J Vibrat Cont* 2016; 23: 3108–3127.
37. Carniel R, Barazza F, Tárraga M, et al. On the singular values decoupling in the singular spectrum analysis of volcanic tremor at Stromboli. *Nat Hazard Earth Syst Sci* 2006; 6(6): 903–909.
38. Rangelova E, Sideris MG and Kim JW. On the capabilities of the multi-channel singular spectrum method for extracting the main periodic and non-periodic variability from weekly GRACE data. *J Geodynam* 2012; 54: 64–78.
39. Hsieh WW and Wu A. Nonlinear multichannel singular spectrum analysis of the tropical Pacific climate variability using a neural network approach. *J Geophys Res* 2012; 10(7): 903–909.
40. Richman MB. Rotation of principal components. *Int J Climatol* 1986; 6(3): 293–335. DOI: 10.1002/joc.3370060305.
41. Venegas SA, Mysak LA and Straub DN. Atmosphere–ocean coupled variability in the South Atlantic. *J Climate* 1997; 10(11): 2904–2920.
42. Groth A and Ghil M. Monte Carlo singular spectrum analysis (SSA) revisited: detecting oscillator clusters in multivariate datasets. *J Climate* 2015; 28(19): 7873–7893.
43. Huang NE, Shen Z, Long SR, et al. The empirical mode decomposition and the Hilbert spectrum for nonlinear and non-stationary time series analysis. *Proc Royal Soc Lon A* 1998; 454(1971): 903–995.
44. Hazra B, Sadhu A, Roffel AJ, et al. Hybrid time-frequency blind source separation towards ambient system identification of structures. *Comp Civil Infrastruc Eng* 2012; 27(5): 314–332.
45. Peng ZK, Tse PW and Chu FL. An improved Hilbert-Huang transform and its application in vibration signal analysis. *J Sound Vibrat* 2005; 286(1): 187–205.
46. Pakrashi V, Fitzgerald P, O'Leary M, et al. Assessment of structural nonlinearities employing extremes of dynamic responses. *J Vibrat Control* 2016; 24: 137–152.